Chapter 12

WAVE FORCES ON SLENDER CYLINDERS

12.1 Introduction

Chapters 6 through 11 have handled the hydromechanics of large (floating) bodies in the sea. Attention now switches to the hydromechanics of slender cylinders. Examples of such cylinders include the leg or brace of an offshore space truss structure, a pipeline or even an umbilical cable extending down to some form of remotely controlled vehicle.

12.2 Basic Assumptions and Definitions

A slender cylinder in this discussion implies that its diameter is small relative to the wave length.The cylinder diameter, D, should be much less than the wave length, λ; the methods to be discussed here are often usable as long as $\frac{D}{\lambda} <$ about 0.1 to 0.2.

Derivations are done for a unit length of cylinder. Force relationships will yield a force per unit length. This relationship must then be integrated over the cylinder length to yield a total force. The implications of this unit length approach combined with the restriction to slender cylinders is that the ambient water motions in the immediate vicinity of the cylinder are all about the same at any instant in time. This is (assumed to be) true both vertically and horizontally; the spatial variation in the undisturbed flow near a unit length of cylinder is simply neglected. A similar assumption was made for the heaving cylinder in chapter 6, but this is not usually the case with a ship or other large structure as discussed in the previous chapters.

The absence of a spatial variation in the ambient flow as one moves from place to place near the cylinder, makes it possible to characterize the flow in the entire region of the cylinder by the ambient flow at one characteristic location. The axis of the cylinder is chosen as that location; this simplifies the bookkeeping.

The flow around this cylinder segment will be considered to be two-dimensional - quite analogous to strip theory for ships except that the axis of the infinitely long cylinder is not generally horizontal as it was for a ship. Flow components and any resulting forces parallel

[0] J.M.J. Journée and W.W. Massie, *"OFFSHORE HYDROMECHANICS"*, First Edition, January 2001, Delft University of Technology. For updates see web site: http://www.shipmotions.nl.

to the cylinder axis are neglected; all forces are caused by the flow - and later cylinder motion - components perpendicular to the cylinder axis.
The axis system used here is identical to that used for the waves in chapter 5, see figure 5.2. The origin lies at the still water level with the positive z-axis directed upward. The wave moves along the x-axis in the positive direction.
The resulting water motions come directly from chapter 5 as well:

$$u = \frac{\partial \Phi_w}{\partial x} = \frac{dx}{dt} = \zeta_a \omega \cdot \frac{\cosh k\,(h+z)}{\sinh kh} \cdot \cos\left(kx - \omega t\right) \tag{12.1}$$

$$w = \frac{\partial \Phi_w}{\partial z} = \frac{dz}{dt} = \zeta_a \omega \cdot \frac{\sinh k\,(h+z)}{\sinh kh} \cdot \sin\left(kx - \omega t\right) \tag{12.2}$$

These can be simplified for the following discussions, however. Since the location, x, of the cylinder element is more or less fixed, the kx term in the above equations can be dropped. For the moment, it is simplest to consider a vertical cylinder so that equation 12.1 will yield the desired flow velocity. All of this yields an undisturbed horizontal flow velocity given by:

$$u(z,t) = \zeta_a \omega \cdot \frac{\cosh k\,(h+z)}{\sinh kh} \cdot \cos\left(-\omega t\right) \tag{12.3}$$

or at any chosen elevation, z:

$$u(t) = u_a \cos(-\omega t) \tag{12.4}$$

and since $\cos(-\omega t) = \cos(\omega t)$ the sign is often dropped so that:

$$u(t) = u_a \cos(\omega t) \tag{12.5}$$

in which:

$$\begin{array}{rcl} u_a & = & \text{amplitude the wave-generated horizontal} \\ & & \text{water velocity at elevation } z \text{ (m/s)} \\ \omega & = & \text{wave frequency (rad/s)} \end{array}$$

Note that the elevation dependence in equation 12.3 has been included in u_a in 12.4; this dependence is not included specifically in the most of the following discussion.
Since the flow is time dependent, it will have a horizontal acceleration as well. This can be worked out to be:

$$\dot{u}(t) = -\omega\ u_a \sin\left(\omega t\right) \tag{12.6}$$

The acceleration amplitude is thus given by:

$$\dot{u}_a = \omega\ u_a \tag{12.7}$$

Since potential theory describes waves so well, the above relations are assumed to hold for any undisturbed wave flow - even when viscosity is involved.

12.3 Force Components in Oscillating Flows

It is convenient to derive the relationships in this section for a smooth-surfaced vertical cylinder. This restriction will be relaxed later in this chapter, however. Since potential flows are so convenient for computations, this discussion of forces in oscillating flows starts with this idealization. The unit length of cylinder being considered is thus vertical and submerged at some convenient depth below the water surface.

12.3.1 Inertia Forces

Remember from chapter 3 that D'Alembert proved that there is no resultant drag force when a **time-independent** potential flow is present. Here, it is the effect of the **flow accelerations** that is of concern.
Consider first the undisturbed ambient (surrounding) flow without any cylinder in it. According to Newton's second law of motion, accelerations result from forces; this is universally true. Thus, the horizontal acceleration of the ambient flow must be driven by a force in the water which, in turn, must come from a horizontal pressure gradient. This pressure gradient is present, even when there is no cylinder in the flow. By examining the pressure gradient force on a differential 'block' of fluid, one discovers that:

$$\begin{aligned} \frac{dp}{dx} &= \rho \frac{du}{dt} \\ &= \rho \cdot \dot{u} \end{aligned} \tag{12.8}$$

which is nothing more than Newton's second law applied to a fluid.

Given this information, what happens when a cylinder is inserted into this pressure and flow field? This question is answered using an approach which has the advantage of physically explaining the separate contributions of two separate inertia force components; a faster, but less 'transparent' derivation will be given later.

Pressure Gradient Force

One must 'drill a hole' in the ambient pressure gradient field in order to 'insert' the cylinder. For now, the fact that the cylinder wall is impervious is neglected completely; the flow is still undisturbed. Any force which this undisturbed pressure field exerts on the cylinder can be computed by integrating this pressure around the perimeter of the circular hole.
This integral yields, knowing that the cylinder is symmetrical with respect to the x-axis and has a unit length:

$$F_{x1}(t) = 2 \cdot \int_0^{\pi} p(R,\theta,t)\ R\ \cos\theta \cdot 1 \cdot d\theta \tag{12.9}$$

in which $p(R,\theta,t)$ is the undisturbed pressure ($\mathrm{N/m^2}$) on the perimeter of the circle and R is the cylinder radius (m).
The resulting force is computed just as was done in chapter 3, using figure 3.16.
Since the pressure difference across the cylinder at any distance, y, away from the x-axis is:

$$\Delta p = \rho \cdot \dot{u} \cdot \Delta x \tag{12.10}$$

where Δx is the width of the cylinder at distance y from its axis. The integral can be simplified again so that:

$$F_{x1}(t) = 2 \cdot \int_0^{\frac{\pi}{2}} \Delta p(R,\theta,t) \cdot R \cdot \cos\theta \cdot d\theta \tag{12.11}$$

After integrating one gets:

$$F_{x1}(t) = \rho\ \pi\ R^2 \cdot \dot{u}(t) \tag{12.12}$$

In which one should recognize $\pi R^2 \rho$ as the mass, M_1, of fluid displaced by the unit length of cylinder - the mass of fluid one would have 'removed' when 'drilling the hole' in the pressure gradient field.
This inertia force term stems from the pressure gradient already present in the accelerating flow - even before the cylinder was installed. It is equal to the product of the mass of water displaced by the cylinder and the acceleration already present in the undisturbed flow. This force component is fully equivalent to the Froude Krilov force mentioned in chapter 6.

Disturbance Force

The cylinder was not allowed to disturb the flow when F_{x1} was computed; this error is now corrected. Obviously, the cylinder is impermeable; fluid cannot actually flow through the cylinder wall. The cylinder geometry forces the fluid to go around it modifying all the local velocities and thus accelerations. This can only occur if a force is exerted on the fluid, and this force can only come from the cylinder.
Figure 3.12, which can be found in chapter 3, shows how the streamlines diverge and converge around a cylinder in a potential flow. One way to evaluate the extra force causing this total disturbance field is to examine the kinetic energy change caused by the cylinder as was done by [Lamb, 1932]. He evaluated the kinetic energy represented by the entire (disturbed) flow field around the cylinder and subtracted from that value the kinetic energy of the undisturbed flow in the same - theoretically infinite - region. This yields in equation form:

$$E = \int_{cyl.}^{\infty} \int_{wall}^{\infty} \frac{1}{2}\rho \cdot \left[u\left(x,y,t\right)\right]^2 dx \cdot dy - \int_{cyl.}^{\infty} \int_{wall}^{\infty} \frac{1}{2}\rho \cdot u_{\infty}^2(t) \cdot dx \cdot dy \tag{12.13}$$

It is convenient to associate this energy with some sort of equivalent mass, M_2, moving with the ambient (undisturbed flow) velocity, u_∞, so that:

$$E = \frac{1}{2} M_2 \; u_{\infty}^2 \tag{12.14}$$

Lamb discovered that:

$$M_2 = \pi \; R^2 \; \rho \tag{12.15}$$

or that M_2 is simply the mass of fluid displaced by the cylinder segment (just as was M_1) so that:

$$F_{x2} = \pi \; R^2 \; \rho \cdot \dot{u}(t) \tag{12.16}$$

Note that F_{x2} has the same form as F_{x1} and that they both have the same phase as well. F_{x2} is analogous to the part of the diffraction force which was in phase with the ship acceleration in chapter 6.
A thoughtful reader may wonder why this second force component, F_{x2} , was not present in a constant current; after all, that cylinder was then impervious to the flow, too. The answer to this question lies in the fact that F_{x2} does not result from the pattern itself, but rather from its continuous build-up and break-down which occurs only in a time-dependent flow. In a constant current there is no time dependent change and thus no F_{x2}.

Resultant Inertia Force

Potential theory indicates that the resultant force on a fixed cylinder in an oscillating flow is the sum of two terms:

$F_{x1}(t) = \rho\,\pi\,R^2 \cdot \dot{u}_\infty(t)$ from the 'hole' in the undisturbed pressure gradient in the ambient flow. This is also know as the Froude-Krilov force.

$F_{x2}(t) = \rho\,\pi\,R^2\,\cdot \dot{u}_\infty(t)$ from the flow disturbance caused by the impervious cylinder.

The resultant force is then:

$$\begin{aligned} F_I(t) &= F_{x1}(t) + F_{x2}(t) \\ &= 2 \cdot \pi\, R^2\, \rho \cdot \dot{u}(t) \end{aligned} \tag{12.17}$$

Note that because this is still a potential flow, there is no drag force. Also, since there is no circulation, there is no lift, either.

Alternate Direct Calculation Approach

Another, possibly faster way to calculate the flow disturbance force coefficient starts with the potential function for an oscillating cylinder in still water. This approach is completely analogous to that used in chapter 6 to determine the added mass of a floating body. One starts directly with the potential function just as was done there, and uses the Bernoulli equation to calculate the pressure on the cylinder surface and then integrate this as was done in chapter 3 to determine the resultant force.

Experimental Inertia Coefficients

The theoretical value of 2 in equation 12.17, above, is usually replaced by an experimental coefficient, C_M - often called the **inertia coefficient**. Remember that the theoretical value of 2 is made up of 1 from F_{x1} (the ambient pressure field) and 1 from F_{x2}, the flow disturbance caused by the cylinder. In practice the 1 from the ambient pressure field is usually considered to be acceptable; potential theory predicts the water motion in undisturbed waves well. The coefficient from F_{x2} is much less certain; the vortices in the wake (in a real, [not potential!] flow) disturb the theoretical flow pattern used to determine F_{x2}. This is taken into account by using a value C_a - a '**coefficient of added mass**' - instead. Usually $C_a < 1$. Note that C_a is quite analogous to the hydrodynamic mass used in chapter 6. This is all summarize in the table below.

Force Component	Force Term	Experimental Coefficient	Theoretical Value	Experimental Value
Froude-Krylov	F_{x1}	1	1	1
Disturbance	F_{x2}	C_a	1	Usually < 1
Inertia	F_I	C_M	2	Usually 1 to 2

Remember that:

$$\boxed{|C_M = 1 + C_a|} \tag{12.18}$$

and that C_a is associated with flow disturbance.

The phrase '**added mass**' has just been used above, much like it is often used in ship hydromechanics as in chapters 6 through 9. C_a is often interpreted as 'hydrodynamic mass' - some mysterious mass of surrounding fluid; this interpretation can be very misleading and dangerous, however. Consider the following true situation taken from ship hydromechanics. An investigator was carrying out tests to determine the hydrodynamic coefficients for a flat-bottomed barge in shallow water. Attention was focussed on its heave motion and the influence of the barge's (relatively small) keel clearance on the hydrodynamic mass. Tests were carried out with various (average) keel clearances so that C_a could be determined as a function of (average) keel clearance value. Figure 12.1 shows a cross-section sketch of the set-up.

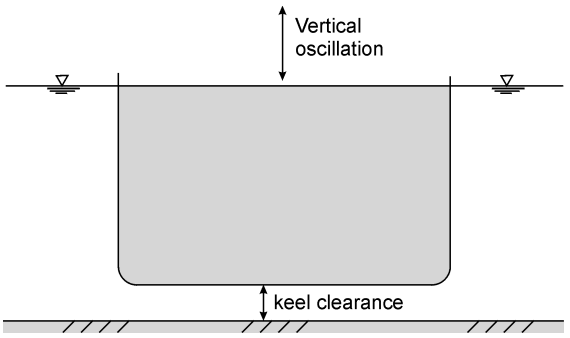

Figure 12.1: Cross Section of Barge Showing Keel Clearance

Since the relatively deeply loaded barge had vertical sides, these caused no waves or other disturbance as the barge oscillated vertically; the only water that is initially really disturbed by the vertical motions is the layer of water directly under the barge. The researcher who carried out these tests then reasoned somewhat as follows: "The mass of water under the ship is directly proportional to the average keel clearance. This mass becomes less and less as the keel clearance becomes smaller; it is therefore logical to expect C_a to approach zero as the keel clearance becomes less and less." His experiments proved however that C_a values became larger and larger as the keel clearance decreased.

The error here is the interpretation of C_a as if it represents a physical mass. It is not this! Instead, C_a (or even C_M for that matter) should be interpreted as force per unit acceleration or $\frac{Force}{Acceleration}$. Returning to the experiments and the researcher above, C_a only represents an 'extra' (in comparison the situation in air!) force needed to given the barge a unit acceleration in the vertical direction. Thinking in this way, one can easily reason that as the layer of water under the barge became thinner, it became more difficult for it to 'get out of the way' by being accelerated horizontally as the barge accelerated downward. Conversely, it therefore took a larger force to give the barge its unit of vertical acceleration as the keel clearance became smaller. With this reasoning, one gets the correct answer: In the limit, $C_a \to \infty$ as the keel clearance $\to 0$.

Fixed Cylinder in Waves

For a fixed cylinder in waves, one is confronted with both F_{x1} and F_{x2} so that equation 12.17 becomes:

$$\begin{aligned} F_I(t) &= F_{x1}(t) + F_{x2}(t) \\ &= \rho \frac{\pi}{4} C_M \, D^2 \cdot \dot{u}(t) \end{aligned} \tag{12.19}$$

in which:

$F_I(t)$	=	inertia force per unit cylinder length (N/m)
ρ	=	mass density of the fluid (kg/m^3)
C_M	=	dimensionless inertia coefficient (-)
$\dot{u}(t)$	=	time dependent undisturbed flow acceleration (m/s^2)

C_M has a theoretical value of 2 in a potential flow.

Oscillating Cylinder in Still Water

One might reason that the flow around an oscillating cylinder in still water would be kinematically identical to that of an oscillating flow past a fixed cylinder and that the resulting forces would be identical. This is not the case, however.
There is no ambient dynamic pressure gradient present in still water so that the first inertia force term above, F_{x1} the Froude-Krilov force, is now identically equal to zero. Thus, if the cylinder is oscillating such that its velocity is given by:

$$\dot{X}(t) = a \cos(\omega t) \tag{12.20}$$

then the resultant hydrodynamic inertia force on the cylinder will be:

$$F_I(t) = -F_{x2}(t) = -C_a \cdot \pi \, R^2 \, \rho \cdot \ddot{X}(t) \tag{12.21}$$

The minus sign indicates that the hydrodynamic resisting force is opposite to the direction of cylinder acceleration. The value of C_a will generally not be larger than its theoretical value of 1. Note as well that if one is measuring forces within an instrumented pile on a segment of this oscillating (accelerating) cylinder, one will usually also measure a force component proportional to the mass times acceleration of the (solid) cylinder element itself. Force measurements in the lab are often corrected for this by first measuring forces while oscillating the cylinder in air before the basin is filled with water. This force is usually considered to be the inertia force of the measuring element itself. Only a slight error is made here by neglecting the aerodynamic resistance caused by the accelerating flow pattern in the still air.

12.3.2 Drag Forces

Experiments have shown (see chapter 4) that a drag force proportional to U^2 and the cylinder diameter, D, is caused by a constant current; it is only reasonable to expect a similar force to be present in a time-dependent real flow as well. Since the drag force is in the same direction - has the same sign - as the velocity in an oscillating flow, the constant

current, U^2, is commonly replaced by its time-dependent counterpart, $u(t)\,|u(t)|$ in order to maintain a proper sign. Substituting relationships for $u(t)$ and working this out yields:

$$F_D(t) = \frac{1}{2}\,\rho\,C_D\,D\,u_a^2 \cdot \cos(\omega t)\,|\cos(\omega t)| \tag{12.22}$$

in which:

$F_D(t)$	=	drag force per unit length of cylinder (N/m)
C_D	=	dimensionless drag coefficient (-)
D	=	cylinder diameter (m)
u_a	=	water velocity amplitude (m/s)
ω	=	circular water oscillation frequency (rad/s)
t	=	time (s)

One should not, however, expect the values of C_D for an oscillating flow to correspond with those found in chapter 4 for a constant flow. Instead, they will have to be determined again in a time-dependent flow.

12.4 Morison Equation

J.E. Morison, a graduate student at the University of California at the time, wanted to predict wave forces on an exposed vertical pile; see [Morison et al., 1950]. He simply superimposed the linear inertia force (from potential theory and oscillating flows) and the adapted quadratic drag force (from real flows and constant currents) to get the following resultant force (per unit length):

$$F(t) = F_{inertia}(t) + F_{drag}(t) \tag{12.23}$$

or:

$$\boxed{F(t) = \frac{\pi}{4}\,\rho\,C_M D^2 \cdot \dot{u}(t) + \frac{1}{2}\,\rho\,C_D D\,\cdot u(t)\,|u(t)|} \tag{12.24}$$

in which the first of these two terms is the inertia force and the second represents the drag force.
Note that in equations 12.24 the drag and inertia force components are 90° out of phase with each other when seen as functions of time. This is a direct consequence of the phase shift between velocity and acceleration in an oscillatory motion; check equations 12.4 and 12.6 if necessary. Examples of this will be shown during the discussion of coefficients and their determination below; see figure 12.2 later in this chapter as well.

12.4.1 Experimental Discovery Path

Morison formulated his equation simply by hypothesizing that the superposition of two separate and well know phenomena (drag in a current and hydrodynamic inertia in an accelerating flow) would yield a viable solution for a vertical pile in waves. This section explains how one comes to the same equation via experiments much like those for ships.
Readers should know from earlier chapters that a common technique in marine hydrodynamics is to oscillate a body with a chosen displacement amplitude in still water and to

record its displacement and the force, $F(t)$ acting on it as functions of time. Further, the force record is resolved into two components: one in phase with the acceleration and one in phase with the velocity.
The first is determined by multiplying $F(t)$ by $-\cos(\omega t)$ and integrating the result to get an inertia force; the second comes from the integral of the product of $F(t)$ and $\sin(\omega t)$ to yield a component in phase with velocity.

One single test might not tell too much, but if testing were done with different excitation amplitudes, but at constant frequency (or period), then a plot of the amplitude of the inertia force component versus the oscillation acceleleration amplitude would be linear; the plot of the drag force amplitude as a function of velocity amplitude would be quadratic. Similarly, comparison of test results carried out with cylinders of different diameter would show that the inertia force component was proportional to D^2, while the drag force would be linearly proportional to D.

Putting all this together would indicate that the force on a cylinder was of the form:

$$F(t) = A \cdot D^2 \cdot \dot{u}(t) + B \cdot D \cdot [u(t) \cdot |u(t)|] \tag{12.25}$$

in which A and B are constants. It is then simple enough to use dimensional analysis and common sense to express the unknown coefficients, A and B as:

$$A = \frac{\pi}{4}\,\rho \cdot C_a \qquad \text{and} \qquad B = \frac{1}{2}\,\rho \cdot C_D \tag{12.26}$$

12.4.2 Morison Equation Coefficient Determination

In this section, a vertical cylinder is assumed to be fixed in a horizontal sinusoidal oscillatory flow. The force per unit length acting on the cylinder can be predicted using the Morison equation with two empirical coefficients:

$$\boxed{F(t) = +\frac{\pi}{4}\,\rho\, C_M\, D^2 \cdot \dot{u}(t) + \frac{1}{2}\,\rho\, C_D\, D \cdot u(t)\,|u(t)|} \tag{12.27}$$

The values of the dimensionless force coefficients C_D and C_M can be determined experimentally in a variety of ways. The first step, however, is always to get a recording of the force, F, as a function of time, t. A characteristic of the flow - usually the velocity - will form the second time function.

Experimental Setup

These measurements can be made in a variety of test set-ups.

1. Oscillating flows can be generated in a large U-tube. Unfortunately the flow can only oscillate with a limited frequency range - the natural oscillation frequency for the installation - unless an expensive driving system is installed. An advantage of a U-tube, on the other hand, is that its oscillating flow is relatively 'pure' and turbulence-free. A discussion continues about the applicability of results from such idealized tests in field situations, however. This topic will come up again later in this chapter.

2. A second method is to impose forced oscillations to a cylinder in still water. The flow - when seen from the perspective of the cylinder - appears similar to that in a U-tube but the inertia force is not the same. Review the material above about C_a to understand why this is so.

3. A third possibility is to place a vertical cylinder in regular waves. The waves are generated by a wave maker located at one end of the experimental tank; they are absorbed on an artificial beach at the other end. In this case it is often the wave height (actually the water surface elevation) which is measured as a function of time. The horizontal water velocity and acceleration at the location of the cylinder are in this latter case determined using linear wave theory - see chapter 5:

$$\begin{aligned} u(z,t) &= \frac{\omega\ H}{2} \cdot \frac{\cosh\left[k\ (z+h)\right]}{\sinh\left(k \cdot h\right)} \cdot \cos\left(\omega t\right) \\ &= u_a(z) \cdot \cos\left(\omega t\right) \qquad (12.28) \\ \dot{u}(z,t) &= -\frac{\omega^2\ H}{2} \cdot \frac{\cosh\left[k\ (z+h)\right]}{\sinh\left(k \cdot h\right)} \cdot \sin\left(\omega t\right) \\ &= -\omega \cdot u_a(z) \cdot \sin\left(\omega t\right) \qquad (12.29) \end{aligned}$$

in which:

$\omega = 2\pi/T$	=	wave frequency (rad/s)
$k = 2\pi/\lambda$	=	wave number (rad/m)
z	=	elevation (+ is upward) from the still water level (m)
H	=	wave height (m)
h	=	water depth (m)
T	=	wave period (s)
λ	=	wave length (m)
$u_a(z)$	=	amplitude of horizontal water velocity component (m/s)

Note that even though u_a is now a function of z, this will not really complicate matters when studying the forces on a short segment of a cylinder. The change in u_a over such a short distance can be neglected.

With any of these methods, the resultant force on a section of the cylinder is often measured by mounting that section on a set of leaf springs which are equipped with strain gauges. These - via a Wheatstone bridge circuit and a proper calibration - provide the force record, $F(t)$ to use in conjunction with the measured or computed $u(t)$ and $\dot{u}(t)$.

Data Processing

Once the necessary data time series have been obtained, one is still faced with the problem of determining the appropriate C_D and C_M values. Here, again, one has several options dependent upon the computer facilities available.

Several methods are presented here, primarily for reference purposes:

1. **Morison's Method**
   Morison, himself, suggested a simple method to determine the two unknown coefficients, see [Morison et al., 1950]. His method was elegant in that it was possible to

determine the coefficients without the use of computers. (Computers - if available at all - were prohibitively expensive when he did his work.) His approach was suitable for hand processing and depended upon the realization that when:
u is maximum, $\dot{u}$ is zero so that at that instant, t_1, $F(t_1) = F_D$ and
$\dot{u}$ is maximum, u is zero so that at that instant, t_2, $F(t_2) = F_I$.
Figure 12.2 shows a sample of an idealized measurement record. Under each of the above specific conditions, equation 12.27 can be re-arranged to yield:

$$\begin{aligned} C_D &= \frac{2F}{\rho D \cdot u_a |u_a|} && \text{at an instant } t_1 \text{ when } \dot{u} = 0 \\ C_M &= \frac{4F}{\pi\ \rho\ D^2 \cdot \omega\ u_a} && \text{at an instant } t_2 \text{ when } u = 0 \end{aligned} \tag{12.30}$$

The method is simple, but it lacks accuracy because:

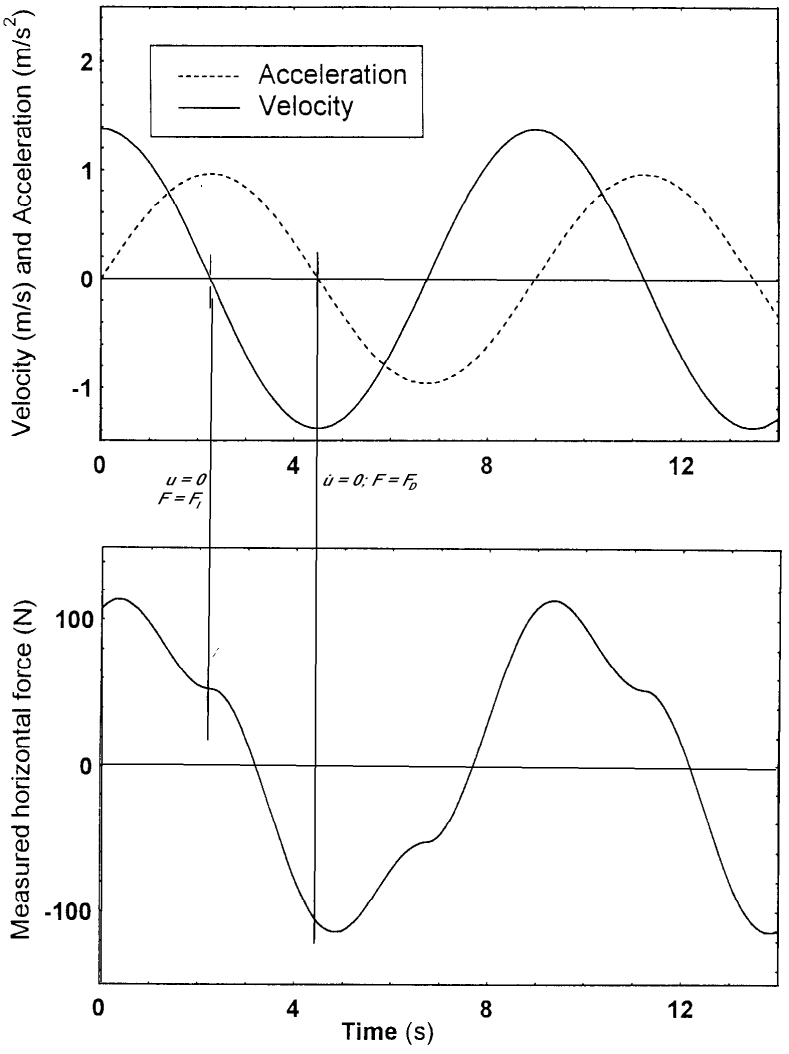

Figure 12.2: Measured Force and Velocity Record

- A small error in the velocity record can cause a significant phase error. Since the

curve of $F(t)$ can be steep (especially when determining C_D in figure 12.2), this can cause quite some error in this coefficient. The effect on C_M is usually smaller.
- Information from only two instants in the time record is used to determine the coefficients; the rest is thrown away.
Morison reduced errors by averaging the coefficients over a large number of measurements (wave periods).
One might try to use this same approach at other time instants in the record. The only difficulty, however, is that one is then confronted with a single equation (for F at that instant) but with two unknown coefficients. This cannot be solved uniquely. A second equation could be created by examining the situation at a second, independent time instant. A generalization of this would be to use the data pairs at every instant with a least squares fitting technique. This is discussed below, but only after another approach using Fourier series has been presented.

2. **Fourier Series Approach**
An entirely different method for determining the drag and inertia coefficients is based upon the comparison of similar terms in each of two Fourier series: One for the water motion and one for the force. Appendix C summarizes the theory behind Fourier series.
Since modern laboratory data records are stored at discrete time steps (instead of as continuous signals), the integrals needed to evaluate the Fourier coefficients are replaced by equivalent sums.
Looking at this in a bit more detail, the water velocity and acceleration is already in a nice form as given in equation 12.28. A single Fourier series term is sufficient to schematize this quite exactly. Since the inertia force, F_I, is also well behaved, it can be 'captured' with a single Fourier series term as well.

The only remaining problem is the series development of the drag term; this requires the development of a function of form:

$$f(t) = A \cos(\omega t) \cdot |\cos(\omega t)| \tag{12.31}$$

This has been worked out in Appendix C as well. The resulting coefficients (given there as well) for the first harmonic development of the quadratic drag turn out to be:

Fourier Coefficient	Value
Constant, a_0	0
Cosine, a_1	$\frac{8}{3\pi} \cdot A = 0.849 \cdot A$
Sine, b_1	0

As shown in Appendix C, the drag force, dependent upon $u\,|u|$, develops into a series of odd-numbered harmonics in a Fourier series; only the first harmonic terms are used here. Since this has an amplitude of $\frac{8}{3\pi}$ times the original signal, one must multiply the first order harmonic of the force in phase with the velocity by a factor $\frac{3\,\pi}{8}$ to get the amplitude of the quadratic drag force.
Once this has been done, then the determination of C_D and C_M from the analysis of the compete force signal, $F(t)$ is completely straightforward. Since the inertia force component shows up now in the b_1 term of the series development, the results are:

$$C_D = \frac{3\,\pi}{4\,\rho\,D} \cdot a_1 \qquad \text{and} \qquad C_M = \frac{4}{\pi\,D^2\,\rho} \cdot \frac{b_1}{\omega\,u_a} \tag{12.32}$$

in which the following amplitudes are found:

$$\begin{aligned} a_1 &= \text{velocity-dependent Fourier amplitude (kg/m}^2\text{)} \\ b_1 &= \text{acceleration-dependent Fourier amplitude (N m)} \end{aligned}$$

Notice that with this method one has used data from the entire time record in the determination of the Fourier series components and thus for the determination of C_D and C_M. This should be an improvement over the method used originally by Morison, but on the other hand, it is still only as accurate as the linearization can be.

3. **Least Squares Method**
A third approach treats the basic Morison equation, (12.27) as a computational approximation, $F(t, C_D, C_M)_{computed}$, for the measured force record, $F(t)_{measured}$. One is now faced with only the problem of determining the (linear) unknown coefficients, C_D and C_M. This is done by minimizing some residual difference (or fit criterion) function. The method of least squares uses a residual function of the form:

$$R(C_D, C_M) = \int_0^T \left[F(t)_{measured} - F(t, C_D, C_M)_{computed}\right]^2 dt \qquad (12.33)$$

in which T is now the length of the measurement record.
Now one only needs to iteratively evaluate equation 12.33 for various values of C_D and C_M until the residual function, $R(C_D, C_M)$ is minimized. If one were to plot this function in three dimensions - with C_D and C_M on the two orthogonal horizontal axes and $R(C_D, C_M)$ on the vertical axis, then one would find a sort of 'bowl-shaped' function. It doesn't take too much thought to realize that if the shape of the bottom of this 'bowl' is rather flat, then there are many combinations of C_D and C_M which give about the same $R(C_D, C_M)$ function value. The consequence of this is that it is quite difficult to determine the 'best' C_D and C_M values exactly in a numerical way. On the other hand, it is theoretically possible to determine the minimum of the function .$R(C_D, C_M)$ by setting both of its partial derivatives, $\frac{\partial R}{\partial C_D}$ and $\frac{\partial R}{\partial C_M}$ equal to zero analytically.

4. **Weighted Least Squares Method**
The least squares method, above, uses the entire time record for the determination of C_D and C_M ; it shares that advantage with the Fourier series approach. On the other hand, one can reason that for offshore design purposes, it is more important that the Morison equation **predict the force peaks accurately** than to be as precise at moments when the force is nearly zero. One way to improve the fitting near the peak forces is to weight the difference found above in equation 12.33 with - for example - the measured or computed force value. Equation 12.33 can then become something like:

$$R_w(C_D, C_M) = \int_0^T \left[F(t)_{measured}\right]^2 \cdot \left[F(t)_{measured} - F(t, C_D, C_M)_{computed}\right]^2 dt$$

Of course the shape of the residual function - the shape of the 'bowl' - will now be different and hopefully steeper and deeper (not so flat on its bottom). Even if this

is not the case, however, one can expect that a Morison equation fitted in this way will give a more accurate prediction of the force peaks.
Note that most any researcher can dream up his own residual or criterion function to use in this approach. Residual values are usually **not dimensionless quantities**; **the absolute (numerical) value** of R or R_w (or any other criterion function for that matter) **is quite irrelevant**; only relative values are of interest. There is certainly no point in comparing them by, for example, comparing values of R with those of R_w. The only important matter is that of finding the C_D and C_M associated with the minimum value of the criterion function chosen.

5. **Alternative Approach**
This method illustrates an entirely different approach to the problem. It was used by Massie some years ago - in an age when digital computers were still slow enough to make numerical integrations a cumbersome process. Instead, integrations were carried out using an analog computer; this could carry out these nearly instantly and painlessly. The analog computer was coupled to a digital computer which read the results of the integration and adjusted the coefficients accordingly for the next try. Such a computer was called a hybrid computer.
The solution was based upon the following approach: First the Morison equation, 12.27, was written in the following form:

$$F(t) = +P \cdot C_M \cdot \dot{u}(t) + Q \cdot C_D \cdot u(t) \cdot |u(t)| \tag{12.34}$$

in which P and Q are simply known constants. Both $u(t)$ and $F(t)$ had been measured and were known functions of time.
The special approach feature was to re-arrange equation 12.34 by solving it for $\dot{u}(t)$ yielding:

$$\dot{u}(t) = \frac{1}{P} \cdot \frac{1}{C_M} F(t) - \frac{Q}{P} \cdot \frac{C_D}{C_M} \cdot u(t) \cdot |u(t)| \tag{12.35}$$

Equation 12.35 is, thus, a first order nonlinear ordinary differential equation in $u(t)$ which has a given solution - the measured $u(t)$ - but two unknown coefficients: $1/C_M$ and C_D/C_M. Values for the unknown coefficients were set by the digital portion of the computer; the analog portion integrated the differential equation to generate a computed $u_c(t)$ and simultaneously subtract it from the measured $u(t)$ to give a residual which was also integrated over a time period in the analog portion. This integral value was the residual function to be minimized using a numerical routine in the attached digital computer. Notice that the criterion function is now based upon the velocity record instead of the force record! Of course, various weighting functions were tried as well.

Five different methods of determining C_D and C_M (or C_a) coefficient values from a single time record of water motion and force have been presented here. The frustrating result of all this is that if one time record were to be analyzed with each of these methods, each method would yield a different pair of C_D and C_M coefficient values! One can conclude - correctly! - from this that it is impossible to determine exact values for these coefficients; a tolerance of several percent is the very best one can expect.

It can also happen that one finds widely varying values for C_D or C_M when comparing results from two different time series with very similar test conditions. This can happen

with the drag coefficient, for example, when $F(t)$ is **inertia dominated** as it is called. Inertia dominated implies that the drag force is relatively unimportant so that since the rest of the information used to compute F_D is relatively small, this small value times any coefficient value is still small. The converse is obviously also true: The inertia coefficient value is unimportant if the force is **drag dominated**. More about the conditions which can lead to this will be presented below in the discussion of the relative amplitudes of the drag and inertia forces.

Cylinder Roughness

All of the above discussion has been for a smooth-surfaced (vertical) cylinder. Since offshore structures accumulate marine growth very easily in at least the warmer seas, this modifies the hydrodynamic force computation in two ways: First, the cylinder can become larger - a marine growth layer of 10 centimeters thickness will increase the cylinder's diameter by 0.2 meters. This can be accounted for quite easily in the Morison equation. The second influence is that the roughness will influence the boundary layer and vortex separation near the cylinder. The drag and inertia coefficient values are generally adjusted to account for this as will be seen later in this chapter.

Presentation Parameters

Now that C_D and C_M values have been found for a given flow condition, it is logical to want to present these results via a graph in which C_D and C_M are the dependent variables plotted along the vertical axis. One must still choose a proper independent variable for the horizontal axis, however. This would (ideally) include information on the wave (H, T or something related to these), the fluid (ρ, ν for example) and the cylinder (D is most obvious choice for this, but it might include the roughness, too). Several possibilities for making dimensionless combinations are discussed in this section.

1. **Reynolds number**
   The Reynolds number for a constant current was given in chapter 4. This is modified here for unsteady flow by replacing the constant current by the amplitude of the oscillation velocity yielding:

$$Rn = \frac{u_a \cdot D}{\nu} \tag{12.36}$$

   in which:
   Rn = Reynolds number (-)
   u_a = flow velocity amplitude (m/s)
   D = cylinder diameter (m)
   ν = kinematic viscosity (m^2/s)

2. **Froude Number**
   The Froude number can now be expressed using the velocity amplitude as well as:

$$Fn = \frac{u_a}{\sqrt{g \cdot D}} \tag{12.37}$$

   in which:
   Fn = Froude number (-)
   g = acceleration of gravity (m/s^2)

The Froude number is associated primarily with free surface effects while wave forces can be exerted on cylinder elements which are so far below the sea surface that no surface disturbance is generated. The Froude number is not really suitable for the present purpose, therefore.

3. **Keulegan Carpenter Number**
[Keulegan and Carpenter, 1958] determined C_D and C_M values for various cylinders in an oscillating flow. They discovered that their data could be plotted reasonably as a function of the dimensionless Keulegan Carpenter number:

$$\boxed{KC = \frac{u_a \cdot T}{D}} \tag{12.38}$$

in which:
KC = Keulegan Carpenter number (-)
T = oscillating flow period (s)
This number can be defined in alternate ways. In a sinusoidal wave, $u_a = \omega \cdot x_a$, in which x_a is the (horizontal) water displacement amplitude. A bit of substitution then yields:

$$KC = 2\pi \cdot \frac{\text{water displacement amplitude}}{\text{cylinder diameter}} = 2\pi \frac{x_a}{D} \tag{12.39}$$

which is very likely an important characteristic for the wake formation in the flow as well.
In **deep water**, the water displacement amplitude x_a **at the sea surface** is identical to the wave amplitude. This allows still another form in this specific situation:

$$KC = \pi \cdot \frac{H}{D} = 2\pi \cdot \frac{\zeta_a}{D} \quad \text{(deep water only)} \tag{12.40}$$

4. **Iversen Modulus**
Even before Keulegan and Carpenter did their work, [Iversen and Balent, 1951] suggested:

$$Iv = \frac{\dot{u}_a \cdot D}{u_a^2} \tag{12.41}$$

in which:
Iv = Iversen modulus (-)
$\dot{u}_a$ = flow acceleration amplitude (m/s^2)
Knowing that in a sinusoidal wave $\dot{u}_a = \frac{2\pi}{T}\, u_a$, and by doing a bit of algebra, one can discover that:

$$Iv = \frac{2\pi}{KC} \tag{12.42}$$

KC is more convenient to use in practice, however.

5. **Sarpkaya Beta**
[Sarpkaya and Isaacson, 1981] carried out numerous experiments using a U-tube to generate an oscillating flow. He found that the ratio:

$$\beta = \frac{D^2}{\nu \cdot T} \tag{12.43}$$

was convenient for plotting his data.
Just as with the Iversen modulus, this can be 'processed' a bit to reveal that:

$$\beta = \frac{Rn}{KC} \tag{12.44}$$

so that this is not really anything new, either.

6. **Dimensionless Roughness**
Cylinder roughness is generally made dimensionless by dividing it by the diameter, yielding:

$$\frac{\varepsilon}{D} = \frac{\text{roughness height}}{\text{cylinder diameter}} \tag{12.45}$$

The Keulegan Carpenter number has survived as the most realistic and useful primary independent parameter for plotting C_D and C_M. This is sometimes augmented by using Rn , β or $\frac{\varepsilon}{D}$ to label specific curves, thus introducing additional independent information.

12.4.3 Typical Coefficient Values

Hundreds (at least) of researchers have conducted laboratory tests to determine C_D and C_M coefficients in one way or another and often for very specific situations. In many cases, their objective and/or experimental set-up limited their range of test conditions so that their results are quite restricted, too. Typical results are listed in this section.
The results of Sarpkaya's experiments with smooth cylinders in U-tubes are presented as graphs of the coefficients C_D and C_M as functions of β and KC. Note that in figure 12.3 the horizontal (KC) axis is logarithmic. Individual curves on each graph are labeled with appropriate values of β.
[Clauss, 1992] for example suggests drag and inertia coefficient values given in the following table:

	$Rn < 10^5$		$Rn > 10^5$	
KC	$\mathbf{C}_D$	$\mathbf{C}_M$	$\mathbf{C}_D$	$\mathbf{C}_M$
< 10	1.2	2.0	0.6	2.0
$\geqslant 10$	1.2	1.5	0.6	1.5

Morison Coefficients Suggested by [Clauss, 1992]

Various design codes or rules also specify (or suggest) appropriate values for C_D and C_M. Those published by [DetNorskeVeritas, 1989] or the American Petroleum Institute (API) are the most widely accepted; the DNV suggestions for design purposes are shown in figure 12.4.

The API as well as the SNAME have the simplest approach as listed in the table below:

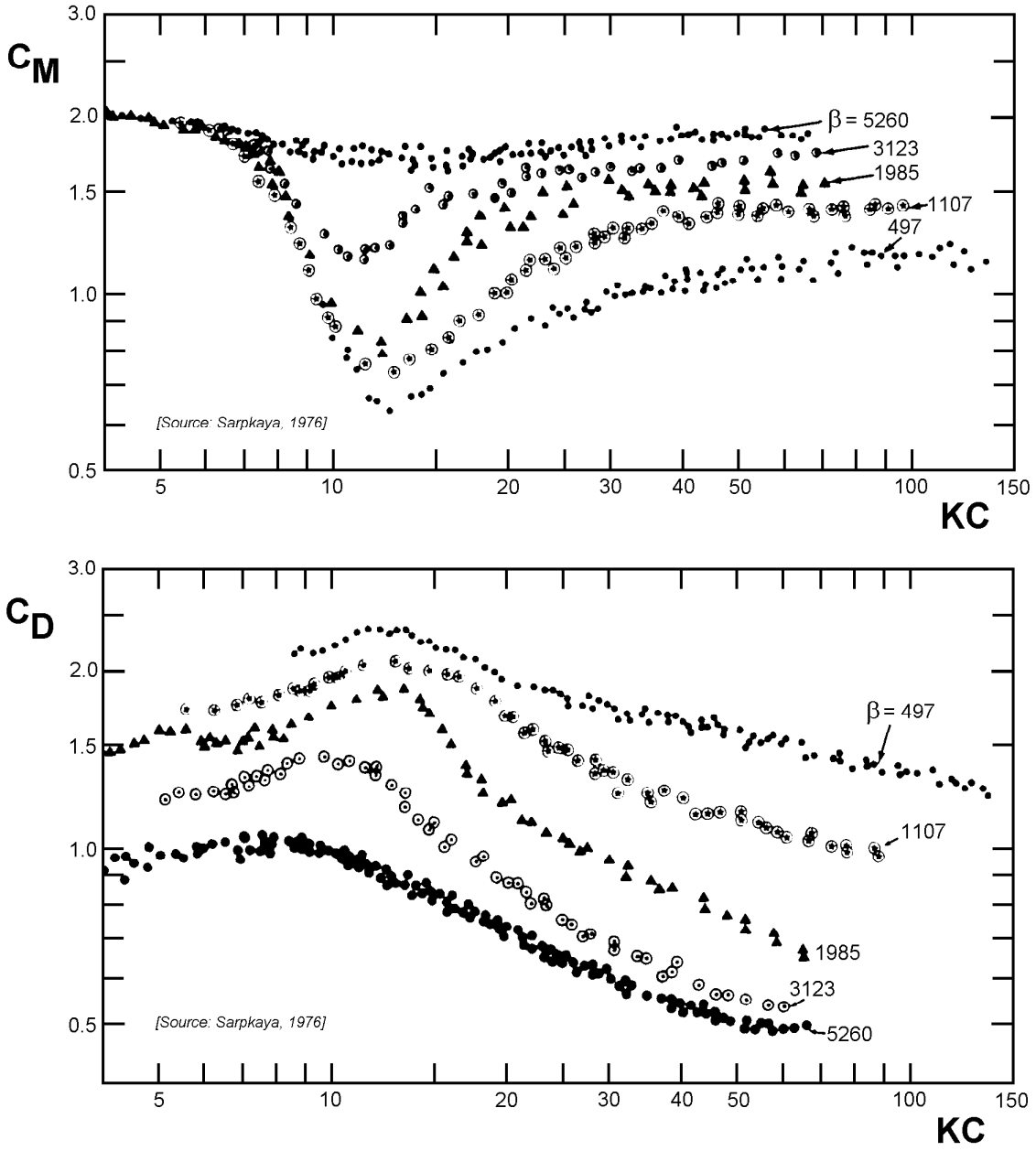

Figure 12.3: Typical Laboratory Measurement Results from Sarpkaya

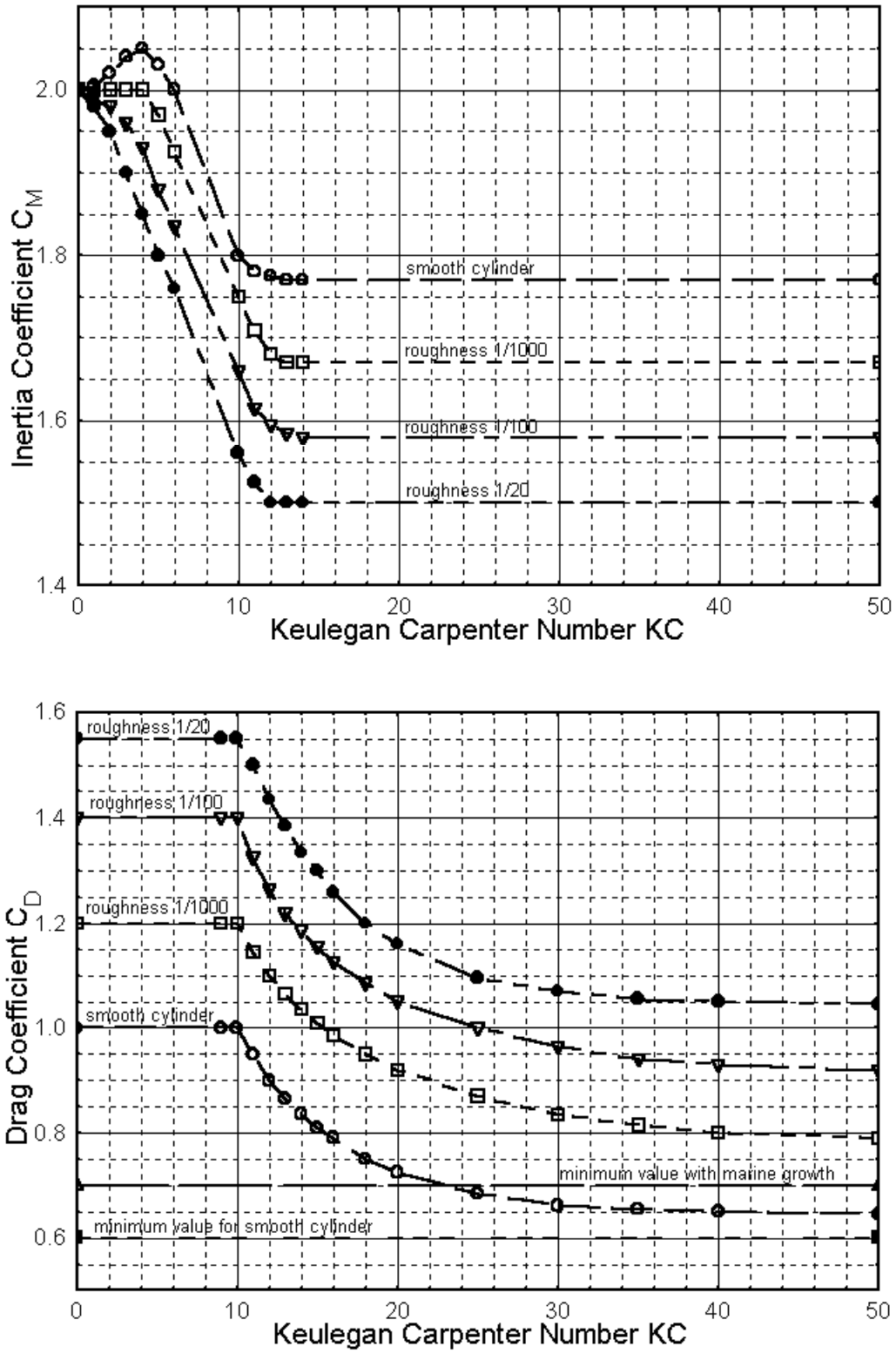

Figure 12.4: Suggested Drag and Inertia Coefficient Values from DNV

	Smooth		Rough	
	$\mathbf{C}_D$	$\mathbf{C}_M$	$\mathbf{C}_D$	$\mathbf{C}_M$
API	0.65	1.6	1.05	1.2
SNAME	0.65	2.0	1.0	1.8

The following observations can be made from the above information:

- For low values of KC, the inertia coefficient C_M is almost equal to its theoretical value of 2 - at least if the KC value is used as a selection parameter. Also, one can notice that the drag coefficient C_D generally increases or stays rather constant till a value of KC near 10 is reached.

- One sees as well from figure 12.3 that the C_D value gets lower as β increases. This is just the opposite of the trend observed with C_M.

- Comparison of Sarpkaya's curves (figure 12.3) with those from DNV (figure 12.4) show that there can be quite some discrepancy in the value of C_D or C_M to choose.

- The DNV curves (figure 12.4) as well as the other design and assessment codes include roughness - that can easily result from marine growth, especially near the sea surface. The roughness in figure 12.4 is an $\frac{\epsilon}{D}$ ratio.

- The API and SNAME recommendations seem rather simple in that they neglect the KC number; Clauss adds that effect, but in a more simple way that suggested by DNV.

Comparisons

Examination and comparison of the various drag and inertia coefficient values presented above shows that there is little agreement on exact values. This is true for smooth cylinder values and even more so when a rough cylinder is involved. Differences of up to roughly 40% can be found when comparing the drag or inertia coefficients suggested by the various sources for a specific flow situation.
This direct comparison of coefficient values can be misleading, however. In some cases a low drag coefficient value can be at least partially compensated by a larger inertia coefficient. After choosing a typical cylinder diameter and wave conditions, one can select appropriate coefficients from each of the sources and compute the actual maximum force per unit length upon which to base a comparison. Such an exercise can still lead to differences of up to about 30%. Luckily for survival design of offshore structures, the differences found for extreme wave conditions are generally less than this!
Even this comparison need not be correct. The 'purest' approach is to select a typical structure, and place it (in one's mind) at a given location in the sea. Given this, one should follow the entire procedure (given in each particular design or analysis code) to select wave and current conditions and to translate these into forces on that structure. These resulting forces should be compared. Carrying out such a comparison operation is beyond the scope of this text, however.
One additional discovery that one will make when computing forces under field conditions is that Sarpkaya's data is a bit restricted for this. Indeed, the Reynolds numbers - needed for his β parameter - are much too low in nearly all laboratory situations.

12.4.4 Inertia or Drag Dominance

Now that C_D and C_M values have been presented, one should further reflect upon their use and importance. The Keulegan Carpenter number can be a very important parameter for this. Indeed, it can be used as an indication of the relative importance of drag versus inertia forces in a particular situation. To prove this, one must work out the ratio of the amplitudes of the drag and inertia forces. The 90° phase difference between the force components is completely neglected now; only the force component amplitudes are compared.

$$\begin{aligned} \frac{F_{drag_a}}{F_{inertia_a}} &= \frac{\frac{1}{2}\,\rho\, C_D\, D\, u_a\, |u_a|}{\frac{\pi}{4}\,\rho\, C_M\, D^2\, \omega\, u_a} \\ &= \frac{2\, C_D\, |u_a|}{\pi\, C_M\, D\, \omega} \end{aligned} \tag{12.46}$$

Note that the maximum value of $|u_a|$ is the same as that of u_a.
Since $\omega = 2\pi/T$, then this can be reduced a bit to:

$$\begin{aligned} \frac{F_{drag_a}}{F_{inertia_a}} &= \frac{1}{\pi^2} \cdot \frac{C_D}{C_M} \cdot \frac{u_a \cdot T}{D} \\ &= \frac{1}{\pi^2} \cdot \frac{C_D}{C_M} \cdot KC \end{aligned} \tag{12.47}$$

Since $1/\pi^2 \approx 1/10$ and the value of C_D is often a bit more than half the C_M value, the two force component amplitudes are about equal when KC is in the range of roughly 15 to 20.
Remembering the earlier definition of KC from equation 12.39:

$$KC = \frac{2\pi\, x_a}{D} \tag{12.48}$$

then this means that x_a/D will be about 3; this is big enough to generate a very respectable set of vortices.

The Morison equation includes a nonlinear (quadratic drag) term which is 90° out of phase with the inertia force. Many offshore engineers want to avoid using the entire Morison equation (and the quadratic drag computation especially) unless it is absolutely necessary. It would be convenient to have a simple way to justify neglecting either the drag term or the inertia term in that equation. The Keulegan Carpenter number is an excellent help with this:

- For low values of KC ($KC < 3$), the **inertia force is dominant**. The flow 'does not travel far enough' relative to the cylinder diameter to generate much of a boundary layer not to mention vortices; potential flow theory is still applicable. **Drag can simply be neglected**.

- For the next range until drag becomes significant ($3 < KC < 15$), one will often **linearize the drag** as has been explained earlier in this chapter.

- There is a range of KC ($15 < KC < 45$) in which one cannot really avoid using the **full Morison equation** with its nonlinear drag.

- For high values of KC ($KC > 45$), the **drag force is dominant**. The vortex shedding frequency becomes high compared to the wave frequency so the flow tends to behave more and more like a uniform flow. **Inertia can be neglected**. Indeed, the limit $KC \to \infty$ corresponds to a constant current.

12.5 Forces on A Fixed Cylinder in Various Flows

This section describes the forces acting on a fixed cylinder in currents and/or waves. While parts of it may seem like repetition of earlier work, its objective is to clarify the underlying principles.

12.5.1 Current Alone

A fixed cylinder in a current alone will experience only a quadratic drag force (per unit length) as already indicated in chapter 4. This force is assumed to be caused by the flow component:

$$U_p = U \sin\kappa$$

acting perpendicular to the cylinder axis so that the force can be expressed as:

$$F_c = \frac{1}{2}\,\rho\, U^2 D\, C_D \sin^2\kappa \tag{12.49}$$

In these equations:

U	=	Total velocity vector (m/s)
U_p	=	Perpendicular velocity component (m/s)
C_D	=	Drag coefficient for constant current (-)
κ	=	Cone angle between the velocity vector, U, and the cylinder axis.
F_c	=	Current force per unit cylinder length (N/m)

See figure 12.5 for a sketch showing the cone angle. The force, F_c, will act in the direction of U_p of course; this is perpendicular to the cylinder axis and in the plane defined by the cylinder axis and the approaching velocity vector, U.
Note that only the so-called cone angle, κ, is important in this computation. This is sufficient to describe the orientation of the cylinder relative to the current vector. It makes no difference whether the cylinder is in a vertical, horizontal or any other plane; it is only the angle between the cylinder axis and total velocity vector which is important. (This will be generalized to include inertia forces in waves below.)

12.5.2 Waves Alone

The time dependent flow associated with waves requires the inclusion of inertia force components into a force computation. Indeed, the basic Morison equation - derived for a unit length of a fixed, vertical cylinder in waves is re-stated here for reference:

$$\boxed{F = \frac{1}{4}\,\pi\,\rho\, D^2\, C_M\, \dot{u}(t) + \frac{1}{2}\,\rho\, C_D\, D\, u(t)\,|u(t)|} \tag{12.50}$$

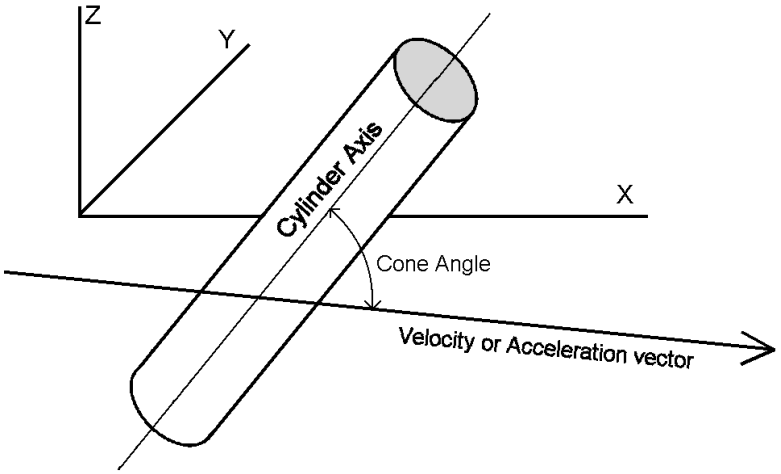

Figure 12.5: Cone Angle Definition

in which:

F	=	Force per unit length of cylinder (N/m)
D	=	Cylinder diameter (m)
$u(t)$	=	Horizontal velocity component (m/s)
$\dot{u}(t)$	=	Horizontal acceleration component (m/s^2)

How can this be generalized in the light of the above information on currents for a cylinder having a non-vertical orientation? The following steps are suggested in which the inertia force and the drag force are considered to be separate entities until the end. The following sequence of steps must be carried out sequentially and at each time step for which results are desired::

1. Determine the instantaneous water kinematics: velocity and acceleration (magnitudes as well as directions) in a fixed x, y, z axis system. Relate their phase to that of a reference such as the wave profile.

2. Knowing the cylinder axis orientation (in that same x, y, z axis system), determine the instantaneous cone angles, κ_I and κ_D for the acceleration and velocity respectively.

3. Determine the instantaneous perpendicular components of acceleration and velocity - $\dot{u}_p$ and u_p - as well as their directions. Use the results from the two previous steps to do this. These two vectors will not generally be co-linear; they are both in the plane perpendicular to the cylinder axis, however.

4. Evaluate the inertia and drag force components at each instant. Don't forget that the drag is quadratic! The direction of each force component will correspond to that of its associated kinematics found in the previous step.

5. If the force on an entire member is needed, then now is the time to integrate these separate force components over the length of the member in order to determine each resultant at that time. The member support forces - and thus the equivalent loads to be applied at the structure nodes - can be found by treating each member as a simple beam.

6. Since the inertia and drag force components are not generally colinear, they can be combined (if desired) via vector addition to yield the resulting force magnitude and its direction (still in a plane perpendicular to the cylinder axis). This step is not absolutely necessary for the computation of resulting forces on a large structure, however.

Note that these five or six steps must be repeated at each instant in time. These steps are not difficult in principle, but very careful bookkeeping is essential!
In many simple cases, each of the quantities needed for this methodology will be expressible in terms of nicely behaved and convenient functions so that the resulting force can be described as one or another continuous time function. On the other hand, if the wave is irregular and thus composed of many frequency and direction components, then the necessary bookkeeping becomes too cumbersome for a hand calculation. The only requirement for the force computation is that the water acceleration and velocity be known at any time.

Special Orientations

One can check his or her understanding of the above by evaluating the forces acting on two special cases of a horizontal cylinder in a regular wave. These are in addition to the vertical cylinder used during the Morison equation derivation.
If the **horizontal cylinder** segment is oriented with its axis **parallel to the direction of wave propagation** (and thus perpendicular to the wave crests), then it will experience a vertical force which has a time trace which looks much like that for a vertical cylinder - see figure 12.2. This force record will be shifted 90° in phase relative to a similar record for a vertical cylinder, however. The relative phases of the resulting drag and inertial force components on consecutive segments of the cylinder will correspond - with some constant shift - to that of the wave profile on the sea surface.
The second case has the **horizontal cylinder** turned **parallel to the wave crests** (and thus perpendicular to the direction of wave propagation). If the cylinder is situated in a deep water wave (in which the horizontal and vertical kinematic components have the same magnitudes) then one will find a resultant force of constant magnitude which sweeps around the cylinder once per wave period. It may seem strange, but the horizontal component of this force will have a purely sinusoidal form (except for a possible phase shift) independent of the fact that quadratic drag is involved. Force components on consecutive segments of this cylinder will have identical phases in this case as compared to the previous one.

12.5.3 Currents plus Waves

It is generally accepted practice to vectorially superpose the current velocity on the velocity resulting from the waves before calculating the drag force. In a general case the wave and current directions will not be co-linear making a vector sum necessary. Once this has been carried out, however, one simply has to use the sequential steps given above to determine the resulting force at any instant.
Why is it not acceptable to compute the wave force and the current force separately? The current has no effect at all on the flow accelerations so that the inertia force is unchanged by the current. The difficulty lies with the quadratic drag force. Since:

$$U_p^2 + u_p^2 < (U_p + u_p)^2 \tag{12.51}$$

then a segregated treatment of the current drag and wave drag - which are superposed only at the end of the computation - will lead to an underestimation of the forces involved.

12.6 Forces on An Oscillating Cylinder in Various Flows

Now that the hydrodynamic interaction of a fixed cylinder in a variety of flows has been explained, it is appropriate to discuss the hydrodynamic interaction of a moving cylinder - again in a variety of flow conditions.
A distinction will now have to be made between the (external) force exerted by the cylinder on the surrounding water and the (internal, structural) force needed to cause the cylinder (segment) to oscillate. In general, the internal force will often be one that is measured - especially in a laboratory setting. This force includes the external hydrodynamic force but also includes a force needed to accelerate the cylinder itself. Also, one should remember that the hydrodynamic interaction force components will generally be in a direction opposite to the actual velocity and acceleration of the cylinder.

12.6.1 Still Water

As indicated much earlier in this chapter, the Froude-Krilov force will be absent since there are no ambient pressure gradients in water which is at rest. The inertia force will be associated with a C_a value and there will be a drag force - associated with C_D as well. Analogous to the assumption made for a fixed cylinder, these forces will be associated with the cylinder kinematics components (velocity and acceleration) which are perpendicular to the cylinder's axis.
The five steps used for determining the forces on a fixed cylinder can used here too, albeit that the kinematics now is that of the cylinder instead of the water.

12.6.2 Current Alone

This interaction situation has already been discussed to some extent in chapter 4. One should remember that the direction of cylinder oscillation and the current direction may be quite different. Indeed, a vortex-induced vibration usually has its largest component more or less perpendicular to the current direction. This results from the lift force - the most important dynamic force in this flow situation - which was discussed in chapter 4.
The drag component of the hydrodynamic interaction was quite well described in section 6 of that chapter too; there is no need to repeat that here.
Inertia forces will - in principle - now be present, too. They will be associated with a C_a value since there is still no ambient time-dependent pressure gradient. These forces will be opposite to the acceleration component which results exclusively from the cylinder oscillation in this case.
In many realistic cases the approaching flow velocity will be considerably larger than the cylinder's oscillation velocity. Also, since most oscillating cylinders are rather slender (an umbilical cable to a ROV is an excellent example) the KC number will be large so that inertia forces will be small anyway. In many practical situations, then, one considers only a drag force as if it were exerted on a fixed cylinder. The drag coefficient is sometimes a bit larger to account for the wider wake resulting from the cylinder oscillation.

12.6.3 Waves Alone

The inertia and drag forces are treated entirely separately here for clarity.

Inertia Forces

Waves will contribute both a Froude-Krilov force (from the ambient, time-dependent pressure gradient) as well as a disturbance force from the encounter with the solid cylinder. The cylinder oscillation, on the other hand, plays no role in the Froude-Krilov force but it does contribute to the disturbance term. (It is implicitly assumed here that the motion of the cylinder is small relative to the wave length so that no phase changes result from this displacement. It is hard to conceive of a practical situation for which this assumption does not hold.) When one keeps in mind that the direction of cylinder oscillation need not coincide with the wave direction, then careful bookkeeping is called for.
One finds the following inertia terms in the equation of motion:

$$M\ \ddot{X}(t) \boxminus C_M\ M_D\ \dot{u}_p(t) - C_a\ M_D\ \ddot{X}(t) \tag{12.52}$$

in which:

M	=	Mass of the cylinder segment (kg/m)
M_D	=	Displaced water mass $= \frac{\pi}{4}D^2\rho$ (kg/m)
$\dot{u}_p(t)$	=	Perpendicular acceleration component from the waves (m/s^2)
$\ddot{X}(t)$	=	Cylinder acceleration (m/s^2)

The symbol $\boxminus$ has been used to segregate terms from the left hand side of the full equation of motion from those on the right. Since only selected terms are included, true equality cannot be guaranteed. The above relationship can be re-arranged by splitting the wave force term into its two components so that:

$$M\ \ddot{X}(t) \boxminus 1\ M_D\ \dot{u}_p(t) + C_a\ M_D\ \dot{u}_p(t) - C_a\ M_D\ \ddot{X}(t) \tag{12.53}$$

If the cylinder acceleration corresponds exactly - in both magnitude and direction - to that of the waves, then the last two terms in this latter equation cancel. This is logical; there is then no disturbance at all and only the Froude-Krilov force remains.
In the more general case, all three hydrodynamic force components in equation 12.53 will be present. It is often convenient to move all the force terms involving the cylinder motion to the left hand side of the equation so that it becomes:

$$(M + C_a\ M_D)\ \ddot{X}(t) \boxminus C_M\ M_D\ \dot{u}_p(t) \tag{12.54}$$

This isolates the (unknown) cylinder motion on the left hand side of the equation and places the time-dependent external exciting force on the right. This right hand side can be evaluated (without knowing the cylinder motion) as a pure time function before the differential equation of the cylinder motion is evaluated.

Drag Forces

Drag forces result from the flow disturbance and wake near the cylinder. Two quite different approaches to the description of hydrodynamic drag are used. They are discussed separately here.

Relative Velocity Approach It is reasonably simple to postulate that this wake depends upon the motion of the water relative to the (moving) cylinder - the relative velocity: $u - \dot{X}$. It results in a drag force proportional to the square of this relative velocity so that one finds the following velocity-dependent terms in the equation of motion:

$$c\ \dot{X}(t) \boxminus \frac{1}{2}\rho\ C_D\ D\ (u_p(t) - \dot{X}(t))\ \left|u_p(t) - \dot{X}(t)\right| \tag{12.55}$$

in which:

c	=	Material damping coefficient ($\mathrm{N \cdot s/m}$)
$u_p(t)$	=	Time-dependent perpendicular water velocity (m/s)
$\dot{X}(t)$	=	Time-dependent cylinder velocity (m/s)

The linear damping term on the left hand side of relation 12.55 involves the internal material damping of the cylinder itself. This has nothing to do with hydrodynamic interaction which is concentrated on the right hand side of the relation.
Notice that the quadratic nature of the drag force makes it impossible to segregate the (unknown) cylinder velocity from the ambient water velocity when computing this exciting force in this way. It is not possible compute this time-dependent excitation force component from the water motion independent of the (also time-dependent) dynamic response of the cylinder. This requires simultaneous step-by-step solution of the differential equation in the time domain. Additionally, an extra iterative loop must be included **within each time step** in order to successively approximate values of $\dot{X}$ until the entire differential equation is satisfied at each time step. This makes such time-domain computations rather time-consuming - even with modern computers.

Absolute Velocity Approach A strict interpretation of this approach uses the principles of superposition in much the same way as they are used in the hydrodynamics of larger structures. The forces resulting from the combined motion of the cylinder in waves plus currents is treated as if it were made up of two independent phenomena: A force caused by the waves plus current on a stationary cylinder proportional to $u_p\ |u_p|$ plus a separate force exerted on a cylinder oscillating in still water which is proportional to $\dot{X}^2$. This approach inherently 'fails to see' the cross product $(-2\ u_p\ \dot{X})$ term included automatically in the relative velocity approach. Further, since the motions of the cylinder will usually be considerably less that those of the surrounding water, the largest contribution to the (external) drag force will therefore come from the $u_p\ |u_p|$ term. This can be left alone on the right hand side of the equation; it can be evaluated quite easily. The relatively small $\dot{X}^2$ term can be linearized and moved to the left hand side of the equation of motion. This linearized drag force now behaves in the same way as a linear damping; it has the same effect as increasing the structural damping which one normally includes in such computations.

Alternatively, one can use an even more pragmatic approach by noticing that the latter two terms of the time-dependent product in the expanded version of relation 12.55 involving u are both smaller than the first term and are often of opposite sign; their combined effect will be small. One now linearizes this small effect and associates it entirely with the cylinder velocity, $\dot{X}$, and treats it as above.

Even if the structure's damping coefficient is not modified, the result of either of these approaches can be that the full differential equation of motion for the cylinder has been

linearized and that the wave-caused excitation force has been isolated on its right hand side. Each motion is treated as if it is in a fixed axis system. It is for this reason that this approach is often referred to as the absolute motion approach.

Comparison Designers tend to be conservative in practice. As a result of this, they tend not to modify the linearized damping when using the absolute motion approach. Since a dynamic system with a lower damping will often have a larger response, the absolute motion approach most usually leads to higher predicted structural responses (internal stresses or even displacements, for example) than does the relative velocity approach. This is indeed a strong motivation to use the absolute velocity approach when evaluating the performance of a proposed design. The additional advantage of having a straightforward and simple computational procedure comes as an added bonus.

12.6.4 Currents Plus Waves

Just as with the fixed cylinder, all hydrodynamic velocity components are generally superposed before starting a force computation. Once this has been done, the further treatment is identical to that for an oscillating cylinder in waves alone as discussed above.

12.7 Force Integration over A Structure

The discussion above has concentrated on the forces on a unit length of cylinder or at least no more than a single member of a large truss structure. It is now time to integrate these forces over the length of the cylinder in order to determine loads which are relevant for structural analysis and design evaluation.
Since many space truss analysis computer programs work with externally applied joint loads, the goal should be to transform the distributed hydrodynamic load on each member of the structure to equivalent concentrated loads at the structure's nodes. Generally, this procedure will have to be followed during a whole series of discrete time steps in order to generate time-dependent loadings which may be needed for a dynamic analysis.
Many computer programs for this purpose work somewhat as follows:
As preparation,

- The nodes of the structure are numbered sequentially.
- Each node is assigned a set of X, Y, Z coordinates corresponding to the intersection point of the member axes at that joint. (Any member eccentricity at the joint is neglected in the hydromechanics.)
- Each member is specified by its diameter and the numbers of the two nodes which it joins. Each member's geometric position and length is now defined.

Once this has been completed the following steps will be carried out for the dynamic loads at each desired time step:

1. The water kinematics - both combined velocities and accelerations - will be computed at each node location. It makes no difference now whether the waves are regular or irregular; there can even be directional spreading or additional currents involved.

The result in all cases is known water kinematics at each node and at every chosen time.

2. If a dynamic calculation is included, and relative velocity drag is used, then the structure's velocity and acceleration at each node will have to be estimated as well. This is usually done by incrementally integrating the structure's equations of motion by working from the previous time step.

3. The results of the above two steps along with the known geometry allow the computation of the force per unit length (for inertia and drag forces separately) at each end of each member. These load intensities will have to be computed separately for each member and at each of its end joints.

4. Most programs now consider each member to be a simple beam carrying a distributed load which is assumed to vary linearly from one end to the other. Note that both the intensity of the loading as well as the vector direction of the loading (about the axis of the cylinder) may vary along its length. (Direction variation can be present when the waves and current are not co-linear. It is also present when wave directional spreading is involved.)

5. Basic mechanics yields the two reaction force components (relative to each member's axis!) at each of its ends.

6. It is now only a matter of bookkeeping to transform these individual member reaction forces into equivalent X, Y, Z force components at each joint.

7. The above X, Y, Z components at each joint are summed to determine the total equivalent applied dynamic load at that joint at the chosen moment. This is the desired result.

8. If relative velocity hydrodynamics is being used this result must be checked. The equations of motion of the structure must be integrated now to determine its new velocity and acceleration at the end of the time step. If these values do no correspond (within a chosen tolerance) with those estimated in step 2, then the above steps must be repeated for another iteration cycle - within this same time step - until the estimated and computed values appropriately coincide.

It is the extra iteration loop discussed in the last of the above steps that makes the relative velocity approach to hydromechanics so computationally inefficient relative to other approaches.
Constant static loads, such as member weight and buoyant forces, can be included in the above computation, but can be computed more efficiently separately before starting on the dynamic computations. The computation principle is analogous to that for the dynamic loads, by the way.

.

Chapter 13

SURVIVAL LOADS ON TOWER STRUCTURES

13.1 Introduction

Chapter 12 has discussed how to compute the hydrodynamic forces on an element (of unit length) of a single (slender) cylinder; a simplified means of estimating the largest hydrodynamic forces on an offshore tower structure will be handled in this chapter.
Figure 13.1 shows an isometric drawing of one of the larger offshore structures. The annotations in that figure will become clear in the course of this chapter.
Some refer to such a structure as a space frame, others see it as a space truss, some just call it a tower. The terms 'frame' and 'truss' have quite different structural engineering connotations which are not at all relevant to the hydrodynamic discussion in this chapter. Another structural distinction is that a jacket is supported from the top by piles driven through its legs while a tower is generally supported from below by piles driven through sleeves - usually at the sea bed. This distinction is also irrelevant for the hydrodynamics being discussed here; the term tower will be used more generically in this chapter to refer to any three-dimensional structure made up from slender elements.
Imagine the bookkeeping and computational effort needed to compute the total hydrodynamic forces on the structure shown in figure 13.1 if this were to be done using the elemental methods of chapter 12. Such a rigorous computation for a 'real' tower structure (with all its members: chords, braces, risers, etc.) is a very cumbersome undertaking, indeed.
Many design engineers have no need for the computational accuracy suggested by a detailed schematization of such a complex offshore structure - at least not during the preliminary design phase. Instead, one more often needs a fast method of making a rough and preferably conservative estimate of the hydrodynamic forces on a complex offshore structure. Such a method can serve two purposes: Give a rough estimate for preliminary design or assure that a detailed model is not making a major error. The objective of this chapter is to outline a 'quick and dirty' method to estimate the horizontal loads on a tower structure. These loads generally yield the largest overall bending moments in the structure and thus axial leg forces as well as the largest horizontal shear forces. These forces and moments are also important for the foundation design. Maximum in-service bracing loads result from

[0] J.M.J. Journée and W.W. Massie, *"OFFSHORE HYDROMECHANICS"*, First Edition, January 2001, Delft University of Technology. For updates see web site: http://www.shipmotions.nl.

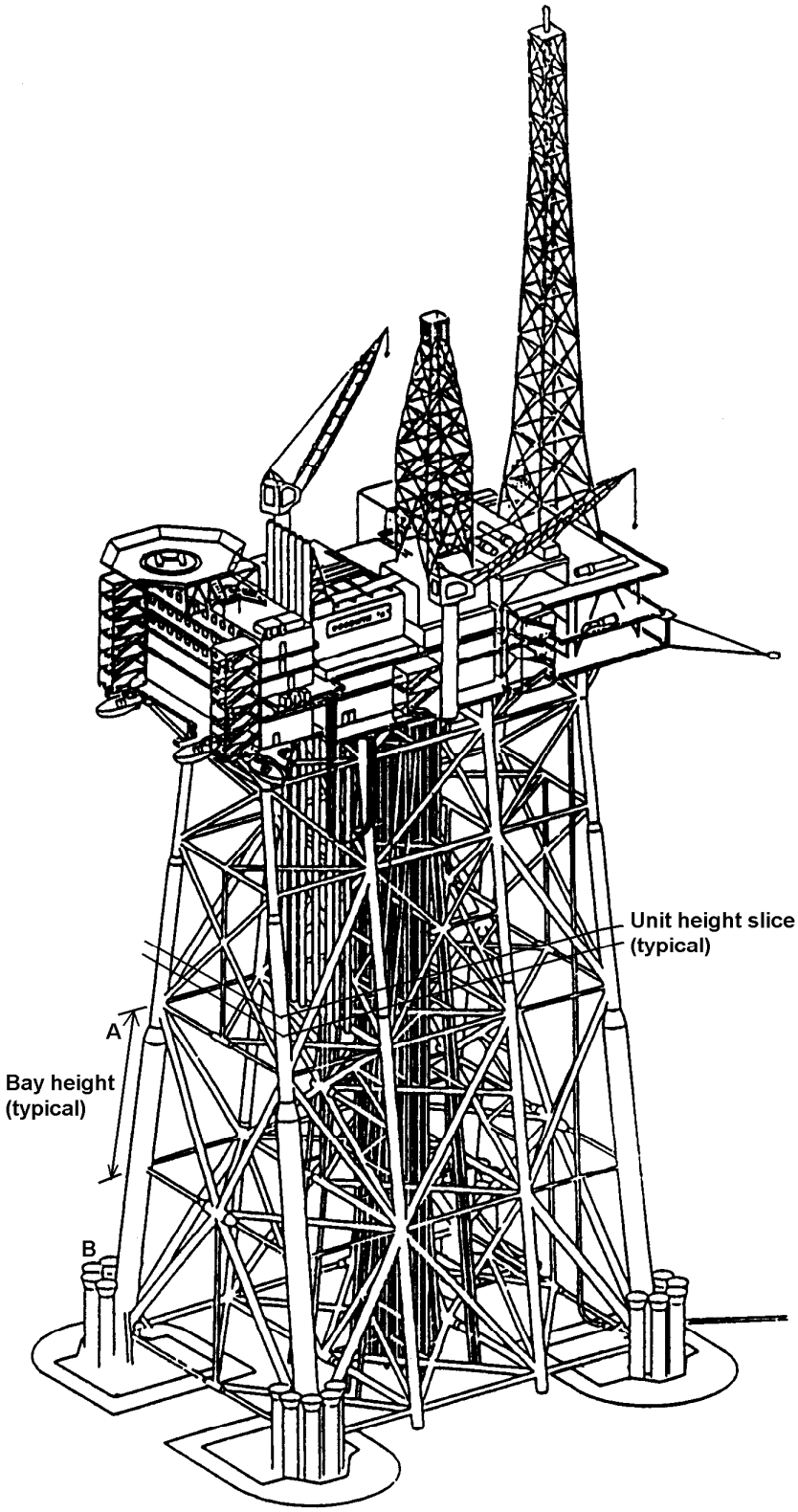

Figure 13.1: Typical Larger Offshore Tower Structure

the horizontal wave and current loads as well.

13.1.1 Method Requirements

The results obtained with any approximation need not be exact - especially if one can reasonably predict whether the 'real' loads will be smaller (or larger) than the estimates. Generally - and for preliminary design in particular - it is handy if the hydrodynamic loads resulting from the approximation are larger than those which would follow from a more sophisticated analysis.
When a preliminary design is based upon loads which are overestimated, it is most likely that the resulting structure will be 'over-designed'; it will be a bit too big, or heavy, or strong and thus probably too costly. Given this fact, then one would not expect the costs of a structure resulting from a more detailed design to come out too high. Said in another way, if the preliminary design survives an economic analysis, then the final design has a good chance of surviving this too - at least to the extent that its total cost is determined by hydrodynamics. An additional factor in practice is that topsides tend to become heavier (as more equipment is added) rather than lighter during the design process. (Whether one likes it or not, topside structures usually tend to get larger and heavier in the course of their detailed design. This can result from equipment or throughput changes as well as from modified environmental or safety requirements.) To the extent that the tower design is dictated by topside weight (if the water is not all that deep depending upon the sea conditions), a bit of initial tower overdesign can prove to be handy during the later, more detailed design analysis phase.
The objective of this chapter, therefore, is to come up with a computational procedure to conservatively predict the hydrodynamic forces on a complex offshore tower structure.

13.1.2 Analysis Steps

Any hydrodynamic analysis of an offshore structure involves the following steps:

1. Selection of environmental conditions (raw data).
2. Schematization of the ambient hydrodynamics.
3. Schematization of the structure.
4. Computation of resulting (survival) forces and overturning moments.

These steps will be followed in the remainder of this chapter.

13.2 Environmental Conditions to Choose

Since one is looking for a maximum external load condition, it is common that this will be caused by a maximum environmental input condition. (A significant dynamic response - which via resonance can lead to enhanced internal loads - can lead to internal response maxima (leg forces, for example) which are caused by more moderate external sea conditions. This is not considered here; it is not that common with tower structures, anyway.) All of this means that extreme wind, wave and current conditions should be chosen for this first design. Each of these involves at least two independent variables: Speed (in some form) and direction. All of environmental inputs can be represented as vectors, but their scalar magnitudes and directions are discussed separately here.

Wind Speed

Wind loads on offshore structures often play a relatively minor role in comparison to the hydrodynamic loads. For an offshore wind turbine, even - on which one would expect to have a relatively high wind load - the wind load is seldom greater than the combined wave and current load unless the structure is placed in water somewhat less than about 20 meters deep (in the North Sea). This implies that the selection of design wind conditions is often not all that important. When one *does* want to estimate wind loads, a maximum one-minute wind gust is often chosen. This wind speed is usually measured at a 'standard' elevation of 10 meters above the sea surface.

Current Speed

Maximum current speeds are usually chosen for survival design purposes as well. One could select a speed corresponding to a maximum spring tide current, for example. In some cases a velocity profile giving the current as a function of depth will be available, too. If not, it is of course conservative to assume that the maximum current acts over the entire depth.

Wave Height and Period

One should choose wave height and period values such that a maximum wave force or overturning moment is obtained. A high wave is obviously needed. If one assumes that the worst part of a storm will have a duration of about 3 to 6 hours and that an extreme wave - if seen as a single wave - will have a period of in the order of 15 to 20 seconds, then one can expect an exposure to something in the order of 1000 waves during the peak of the storm. The highest wave in a series of 1000 would have a chance of exceedance of $\frac{1}{1000}$. Substituting this in a Rayleigh wave height distribution yield a design wave height of 1.86 times the design significant wave height chosen. (If one works out these limits more exactly, one should expect something more than 540 waves and less than 1440 of them; one thousand is pretty close to the average - by chance. If $\frac{1}{540}$ and $\frac{1}{1440}$ are used instead, the wave height ratio is in the range 1.77 to 1.91; this makes no more than 5% difference.) Selecting the shortest wave period consistent with the chosen wave height will yield maximum water velocities and accelerations - at least near the water surface. On the other hand, the hydrodynamics of waves with shorter periods 'die out' faster at deeper locations; a proper balance must be found between these two requirements. Wave breaking will, of course, put a lower limit on the wave period for a given wave height; a very high and very short wave will break so that one should also check any chosen combination of these to be sure that the wave is not broken. The necessary relationships (for deep water and a quick estimate) include:

$$\lambda = 1.56 \cdot T^2 \qquad \text{and} \qquad \frac{H}{\lambda} < \frac{1}{7} \tag{13.1}$$

in which λ is the wave length (m), H is the wave height (m) and T is the wave period (s). The above relations - which come directly from regular wave theory of chapter 5 - are less dependable for larger and irregular waves at sea, however.
Since H will generally be rather large, λ will not be small, either. The significance of this will show up below.

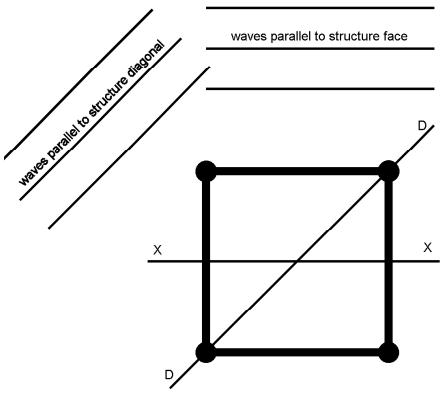

Figure 13.2: Schematic Plan of Tower and Approaching Wave Crests

Wind, Current and Wave Directions

In general, each of these independent physical phenomena will have its own direction, independent - at least to some extent - from that of others. This is most obvious for the relation between the tidal current direction and the wave direction. These seldom have much correlation. The wind direction and the wave direction - in a major storm at least - is usually rather well (but not perfectly) correlated of course.
The conservative choice (which is easy to work with too!) is to simply assume that all three of these phenomena are colinear; they all come from the same direction.
Be sure to keep the direction bookkeeping correct. The wind direction is specified usually as the direction from which it comes, while a current direction is most commonly stated as the direction to which it goes. It sounds inconsistent, but a northwest wind and southeast current go in the same vector direction.

An independent direction consideration involves the orientation of the structure (about its vertical axis) relative to the environmental conditions. Consider a simplified situation as shown in plan in figure 13.2. The solid circles represent the legs of the tower as seen from above. Two possible wave and current approach directions (indicated by the wave crests) are shown: One with crests parallel to a face of the structure (and its X axis) and one with crests parallel to its diagonal - the D axis in the figure. If one assumes for simplicity (for now) that the total external horizontal force as well as the overturning moment about an axis at the sea bed is independent of the approach direction, one will still find larger axial pile forces when the wave crests are parallel to a diagonal. On the other hand, since the horizontal shear forces within the structure are carried primarily by the bracings, waves approaching parallel to one side of the tower will generally lead to maximum forces in these members.This is because the entire shear load is carried by only half of the braces then; braces parallel to the wave crests carry essentially no load.

Phasing

All of the independent environmental phenomena - wind, waves and tides - are time dependent. Do all of the maxima selected above then occur at one and the same instant? Formally, the answer to this lies in a comparison of the periods of the various phenomena. Since the tidal period (12 h 24 min) is long relative to the wind gusts and waves, it is

almost certain that a high wave or strong wind gust can occur when the tidal current is high.
Looking next at the wind gust relative to the wave, its duration (1 minute) would be a few wave periods long. Here, again, there is at least some finite chance that a major wave peak will coincide with this in time. On the other hand, many more waves will occur at times when the design wind gust is *not* present!
Of course, assuming that the maxima of wind, waves and current *do* occur simultaneously will lead to a conservative result; this is chosen here.

Implications

The choices made above already have significant implications for the computations to be carried out. For example, the wave length, λ , chosen above will be rather large relative to the horizontal dimensions of (most) offshore structures being considered. This means that there will be relatively little phase difference between the 'upstream' and 'downstream' sides of the entire structure at any instant in time.
In chapter 12 the phase shift from one side to the other side (of a single cylinder) was neglected. Now, with an extreme wave, the same reasoning is being applied to an entire tower structure. Since phase differences only tend to reduce the horizontal loads on the structure, neglecting these will be conservative. Additionally, neglecting this phase difference will simplify the formulation of the structural model enormously.
Since the wave is relatively high, the Keulegan Carpenter number $KC = \frac{\pi \cdot H}{D}$ (at the sea surface and in deep water) will tend to be high as well. This indicates that the wave forces will tend to be drag dominated - at least at the sea surface where they are largest.
Note that if the structure is not in deep water, the actual KC value will be even higher than that estimated above; this can be checked by using the complete equations - rather than deep water approximations - to describe the water motion. When the current is added to the water velocity caused by the wave, then this drag dominance becomes even more pronounced, of course. In all cases, the water velocity will decrease with depth so that the KC value will decrease as well. One can expect the inertia force to increase in importance as one moves down along the structure. A significant current can prevent it from ever playing much role, however.
Remember too from wave kinematics that the maximum horizontal water velocity in a wave occurs under that wave crest or trough. The total resulting force (integrated over the structure) will be greatest when the wave crest passes by, simply because more of the structure is then exposed to the wave. Wave kinematics will have to be predicted over the entire height from the sea bed to the wave crest in order to carry out such a computation.

13.3 Ambient Flow Schematizations

This section discusses the numerical models needed to translate the raw data on environmental conditions into input data for a force model.

Wind

Wind velocity distributions have been discussed in chapter 4. If - as is standard meteorological practice - the wind is given at a standard elevation of 10 meters above mean sea

level, then wind speeds at other elevations are often predicted from this value by using:

$$\frac{V_{tw}(z)}{V_{tw}(10)} = \left(\frac{z}{10}\right)^{0.11} \quad \text{(at sea)} \tag{13.2}$$

in which:

z	=	desired elevation (m)
$V_{tw}(z)$	=	true wind speed at elevation z (m/s)
$V_{tw}(10)$	=	true wind speed at 10 meters elevation (m/s)

The exponent 0.11 in equation 13.2 is for sea conditions only; see chapter 4.

Some designers often reason that since wind loads on many offshore structures are often relatively unimportant and hydrodynamic loads tend to be over-estimated, they can just neglect wind loads altogether. This is certainly the very simplest approach that can be chosen. On the other hand, the wind load has the longest moment arm when one is studying the overturning moments about the structure's base. It is best not to neglect them in the overturning moment computation at least.

Waves

A maximum wave at sea results from the superposition of a large number of wave spectrum components. The objective here is to replace this multi-component wave with a single regular wave for computation purposes. Linear wave theory is certainly convenient for predicting the water kinematics within such a wave, but it has one important drawback: It predicts water motions only in the zone below mean sea level. As has been indicated above, the water motions right up to the wave crest will have to be predicted. Methods for doing this have been given in chapter 5. Of these, the use of a constant velocity - the same as the velocity at $z = 0$ - or Wheeler stretching are the most popular.
Remember from chapter 5 that the (extreme) wave crest will be higher than $H/2$ above the still water level as well. A common rule of thumb is that:

$$\zeta_{\max} = +\frac{2}{3}\,H \qquad \text{and} \qquad \zeta_{\min} = -\frac{1}{3}\,H \tag{13.3}$$

With this, one can use either constant extension or Wheeler stretching along with the complete equations for the water motion in order to calculate the horizontal components of water particle acceleration and velocity at all elevations between the sea bed and wave crest. All details of this can be found in chapter 5.

One should note the following about the waves formulas to be used:

1. If only a maximum velocity is needed, the time function in the wave can be neglected.
2. Since the wave length is usually considerably larger than the horizontal dimensions of the total structure being considered, the phase relation, kx can be dropped too.
3. If the wave crest is involved, then the maximum crest elevation will follow from equation 13.3.
4. The full equations (and not deep or shallow water approximations) must be used when evaluating the horizontal kinematics in the wave. This is then valid for any water depth and at any point under a wave profile.

Use of deep water wave theory - with its simplifications - can lead to less than conservative results as the water depth decreases; this is the reason that use of the full theory is recommended above.
The wave height used should be the correct one for the actual water depth, h. Include the shoaling influence, if appropriate; see chapter 5. Use this same actual water depth when computing λ as well.

Current

Since the current is constant and in the same direction as the wave propagation, it can simply be added to the velocity component amplitude, $u_a(z)$, computed for the wave. If the current velocity is given by $V(z)$, then the total horizontal velocity will become:

$$U_a(z) = V(z) + u_a(z) \tag{13.4}$$

Of course, $V(z) = 0$ for $z > 0$.

Remark

Upon reflection, one can conclude that the computational effort needed to describe the environmental hydrodynamics and aerodynamics has been simplified considerably in comparison to the most general case:
- Only conditions under the wave crest are considered.
- Only hydrodynamic drag is considered.
- All spatial phase differences are neglected.

These all reduce the computational effort. On the other hand, one is forced to add a limited amount of complication in order to:
- extend hydrodynamics up to the wave crest and
- have a solution valid for all water depths.

Even so, the overall result of all this is that the hydrodynamics has been considerably simplified. A simplified schematization of the offshore structure will be discussed in the following section.

13.4 Structure Schematization

The objective of this section is to replace the actual truss-like marine structure - with all of its members and nodes - with a much simpler and computationally efficient equivalent one for the purpose of estimating its external hydrodynamic drag loads. The formulations derived in this section are valid only when all velocity or acceleration components are co-linear. This means that the all waves and all currents come from the same direction. This is completely in agreement with the schematization of the environment made above, but it will not be true in a more general case. The formulations in this section will be incorrect, however, if the current comes from another direction than the waves or even if only directional spreading of the waves must be included.
The drag term in the Morison equation (for a vertical cylinder) is of the form:

$$F_{drag_a} = \frac{1}{2}\rho\, C_D\, D \cdot U_a^2 \tag{13.5}$$

in which:

F_{drag_a} = drag force amplitude per unit length of vertical cylinder (N/m)
C_D = drag coefficient, to be discussed later (-)
D = cylinder diameter (m)
U_a = horizontal velocity amplitude at the chosen elevation (m/s)

Since U_a will be positive in this case, $U_a \cdot |U_a|$ has been replaced by U_a^2.

Consider now a horizontal 'slice' of the entire structure having a unit height; see figure 13.1. What happens as one sums the drag forces across all the members found at that level? $\frac{1}{2}\rho, C_D$, and U_a in equation 13.5 remain constant. The remaining quantity, D times a unit height, is simply an area. Since attention focuses on the horizontal forces on the structure, this is an area projected on to a vertical plane, perpendicular to the 'slicing' planes; it is the area one would be able to measure on a side view photograph of the structure (if no members were hidden behind others in that photo!). The 'photo' should be made looking in the direction of wave propagation, of course.
Continuing for now with a 'horizontal slice' (of unit height) of the structure at a given elevation, then the equivalent diameter, D_e, which must be used in the Morison equation drag term (in order to get the total drag force) is simply that total area (as seen on the projection or photo) divided by the unit height.
Upon reflection, one will discover that at each elevation, z, one finds the following contributions to D_e:

- Leg chords (nearly vertical) each contribute their actual diameter, D.
- Horizontal braces (if present at the chosen elevation) at an angle θ relative to the plane of water motion contribute:

$$D_e = L \sin\theta \tag{13.6}$$

in which:

L = brace length (to the centerline of its nodes) (m)
θ = brace azimuth relative to the water motion plane (rad)

but only over the limited height, D.

- Sloping braces in the plane of the picture contribute:

$$D_e = \frac{D \cdot L}{H_B} = \frac{D}{\sin\alpha} = D \ \csc\alpha \tag{13.7}$$

in which:

H_B = height of the bracing bay (m); see fig. 13.1
α = slope of brace relative to the horizontal (rad)

- Sloping braces in a vertical plane perpendicular to the plane of the picture (in the plane of the water motion) contribute D.
- Sloping members with other spatial orientations - think of sloping braces when waves approach a tower in a diagonal direction - require a bit more geometry and bookkeeping. Letting:

$$\ell = \frac{1}{2}\left(\frac{L}{H_B} - 1\right) = \frac{1}{2}\left(\csc\alpha - 1\right) \tag{13.8}$$

then:

$$D_e = D \cdot \{1 + \ell \cdot [1 - \cos(2\theta)]\} \tag{13.9}$$

in which θ is the bracing azimuth relative to the wave direction (rad).
This angle θ could alternatively be referred to as the angle between the (vertical) plane which includes the brace and the vertical plane in which the flow takes place. One might note that equation 13.9 is quite general; it even works (in a degenerate way) for a vertical cylinder.

One can argue that measuring each brace length to the centerline of each of its end nodes, includes too much length; more than one member is being counted within each joint's volume. This is true, but it is often seen as a compensation for the fact that the flow will actually be more complex in the joint vicinity. This will - in turn - likely lead to higher forces than would be predicted for a single straight member.

Since the diameter is a linear factor in the drag force relation, one can simply sum the above diameters at any given elevation to come to a total equivalent diameter, $D_e(z)$, to use at that elevation. This procedure reduces the 'forest' of truss and other members at each elevation, z, to a single vertical cylinder segment.
For most structures, the resulting vertical cylinder will look rather 'lumpy' in that its diameter will not be constant over its length. Indeed, whenever horizontal members are encountered, D_e will abruptly bulge out and become larger. It can also be larger where the leg chords become larger or near the sea bed where extra legs or pile sleeves are often included in the structure. Locations A and B in figure 13.1 are such elevations.
Some may wish to simplify this schematization even more by 'smoothing out' these diameter bulges. This can be a dangerous operation, because the hydrodynamic forces are quite elevation-dependent (and structure overturning moments are even more so) - especially in the zone just below the sea surface. This is at best an operation which must be based upon broad experience.

13.5 Force Computation

Now that the environment as well as the structure have been schematized, one is well on his or her way to computing the hydrodynamic forces and associated overturning moment. One remaining preparatory task is to select an appropriate drag coefficient. Usually a single value is chosen for the entire structure.
How should the drag coefficient be selected? One wrong approach is to use the diameter of the schematized pile, D_e, and u_a to compute the Keulegan Carpenter number, KC, and then to select C_D based upon these values. This is wrong because the equivalent cylinder diameter, D_e cannot be found in the sea at all.
The diameter selected for determining C_D should be more representative of those found in the real structure which is being schematized. If one also discovers that C_D is then rather independent of the exact value of KC, then one is extra fortunate; the precise choice of diameter used in this determination is not critical then anyway.
Should u_a or the total velocity, U, be used to compute KC? Usually only the wave-caused velocity component, u_a, is used, but this can be a very interesting discussion topic.

Once a proper C_D value has been selected, then the (peak value of) the drag force per unit elevation can be computed directly:

$$F_{drag_a}(z) = \frac{1}{2}\rho\ C_D\ D_e(z) \cdot U_a^2(z) \tag{13.10}$$

for the waves plus current, and:

$$F_{wind_a}(z) = \frac{1}{2}\rho_{air}\ C_d\ A_w(z) \cdot V_{tw}(z) \tag{13.11}$$

in which $A(z)$ is the projected area exposed to the wind.

13.6 Force and Moment Integration

The drag forces caused by the wind as well as waves and currents are known as a function of elevation. All the necessary information is now available to compute the resulting horizontal force and overturning moment on the (schematized) structure.

13.6.1 Horizontal Force Integration

The resulting horizontal force can now be computed by integrating F_{drag_a} and F_{wind_a} over the appropriate height segment of the structure. This integration can most efficiently be done using a spreadsheet program. This integration usually proceeds by computing the forces (per unit length) at chosen elevations and then linearly interpolating the loading between these values. The elevations to choose for this evaluation should be chosen based upon the following criteria:

- If D_e or A_w changes abruptly, then one should evaluate the loading for each value - just above and just below the transition.
- Additional successive elevations should be chosen close enough together so that linear interpolation between elevations still provides a reasonable approximation of the exponential curve of the actual elevation function associated with the drag force.

The linear interpolation procedure suggested here replaces some form of elevation dependent exponential decay function by a straight line. This is generally conservative and quite in accordance with the objective of overestimating - if anything - the results. In order to prevent this overestimation from becoming too great, one must be sure that the linear function used for a segment of elevation does not diverge too much from the actual elevation decay function. This implies that finer integration steps - shorter (in height) tower slices - should be selected where conditions change rapidly. Sensitive locations can be found near the water surface and wherever the structure changes abruptly.

13.6.2 Overturning Moment Integration

Overall structure overturning moments are usually computed about a horizontal axis at the sea bed (mudline). The computation proceeds quite analogously to that used to compute the horizontal force, but now one must include the appropriate moment arm with each integration step. This is simply the elevation of that segment relative to the sea bed.

Alert readers can (correctly, in theory) point out that when a real structure - with 'real' horizontal dimensions - includes horizontal members (this is usually the case, by the way!), then the *vertical* water motions *also* induce overturning moments about the mudline. Luckily, one only has to sketch the water motion as a wave progresses through the structure to conclude that the vertical velocity components near the wave crest are small and that this additional (small) moment acts counter (in the opposite sense) to that just computed above. Once again, the objective of predicting an upper bound for the overturning moment is achieved by neglecting this small (and very time-consuming!) detail.

13.7 Comparative Example

The 'proof of any pudding is in the eating'; this section demonstrates the results of computations carried out using the various alternative computation procedures. This is illustrated here by working with an arbitrarily chosen standard case and then by varying one a single variable (while keeping all the others constant) in order to observe its influence.
The standard case involves:

Input Item	Value
Wave Ht. H	15 m
Wave Per. T	12 s

as a wave whose crest extends 10 meters above the still water level. This yields a q parameter for the Wheeler Stretching of 0.80. Further, in order to focus the comparisons on the hydromechanics and to avoid a discussion of the structure or the drag coefficient, the following quantity is keep constant from the wave crest elevation (+10 m) to the sea bed.

$$\frac{1}{2}\rho C_D D = 1000 \tag{13.12}$$

Further, only the drag force is considered here.
Computations have been carried out for each of the four treatments of the splash zone discussed in chapter 5:

- Linear Theory - nothing above the still water level
- Extrapolated Linear Theory - linear theory functions are continued to the wave crest.
- Constant Extrapolation - the linear theory value as $z = 0$ is used for all positive z values
- Wheeler Stretching - the profile is stretched to the wave crest.

Since the water motion in waves is more or less concentrated near the sea surface, one would expect that the total horizontal force on a structure would increase more and more slowly as the water depth continues to increase; each additional increment of structure height (added at the bottom) adds less and less total horizontal force.
As the water depth approaches zero - at the other end of the range - one might reason that the total horizontal force there should also approach zero as the tower height exposed to the waves becomes less and less.

Figure 13.3 shows the total static horizontal shear force at the base of the structure (the integral of the drag force from the wave crest to the sea bed) versus water depth.

The behavior of the curves on the right-hand side of the figure is as expected; the behavior on the left is not - although the curves do not extend completely to a zero water depth. As the water depth decreases, the water motion in the wave becomes more and more like that of a shallow water wave; the horizontal water velocities increase. This increased water velocity - especially when used in a quadratic drag force formula - causes the force per unit height of the structure to increase so rapidly that it more than compensates for the corresponding loss of total tower height. The curves are not extended to zero depth because wave breaking would limit the wave height. Neither wave breaking nor wave height changes resulting from shoaling outside the breaker zone are included in this analysis.

The four curves on the figure are located more or less as one would expect. It is no surprise that extrapolated linear theory yields the largest force and that 'plain' linear theory the lowest.

Figure 13.4 shows the resulting moments. As would be expected, the overturning moment increases significantly with water depth. The relative positions of the four curves is logical as well in view of the results above.

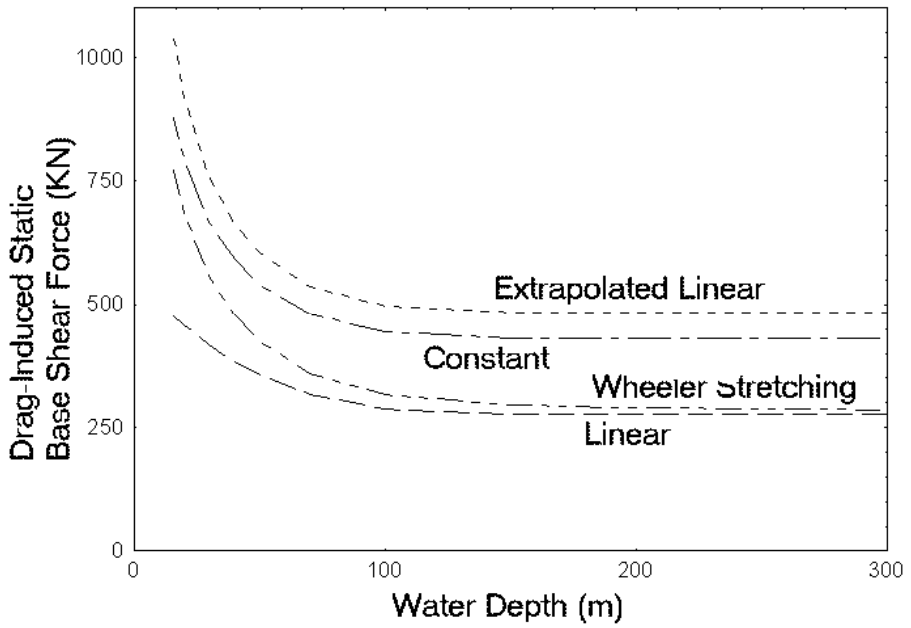

Figure 13.3: Horizontal Force versus Water Depth

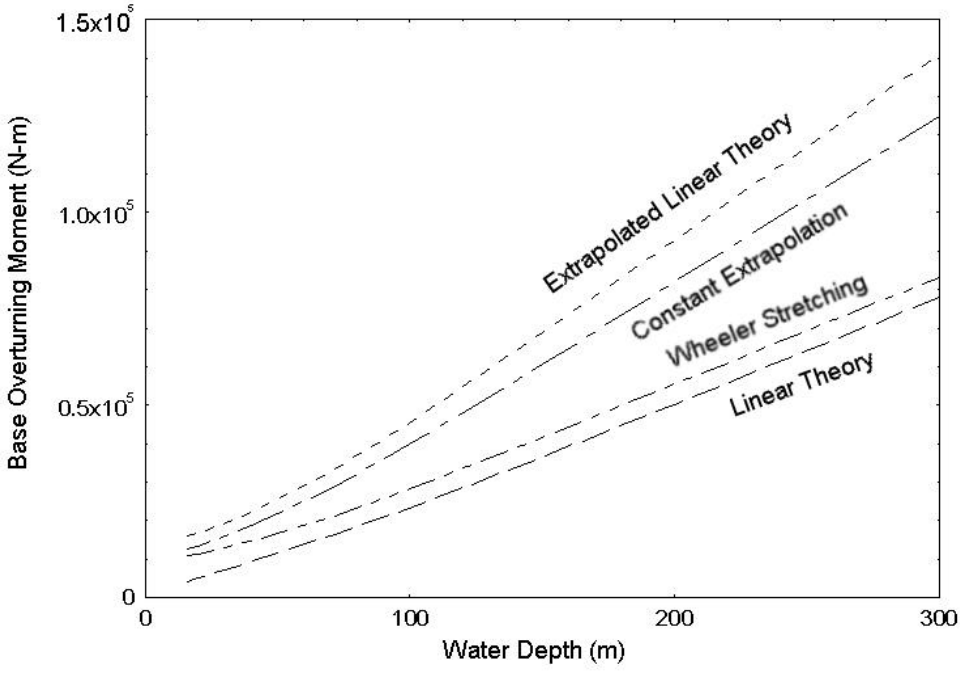

Figure 13.4: Base Overturning Moment versus Water Depth

Chapter 14

SEA BED BOUNDARY EFFECTS

14.1 Introduction

So far, attention has focussed on flows near and forces on man-made objects in the sea. Now, attention is shifted to the largest object in the sea: the sea bed, itself. Along the way, a few topics concerning forces on small man-made structures placed on or near the sea bed will be discussed as well.

These are all cases in which the flow of sea water over the sea bed is markedly influenced by the sea bed boundary layer; an exposed pipeline is an excellent example as is an item of ship's cargo that has been lost overboard and has sunk.

The influence of the flow boundary layer on the sea bed itself becomes important when one considers the erosion or deposition of sea bed material near a man-made object. Erosion around the piles of an offshore platform can leave a segment of the piles without lateral support. It is harder to find and recover a valuable piece of ship's cargo that has become covered by the natural action of the sea bed.

The approach used in this chapter is not, in principle, really any different from that used already. First attention is paid to the flow - in the vicinity of the sea bed, in this case. This is followed by a discussion of forces on objects (including the sea bed itself!) and the consequences which these forces can have.

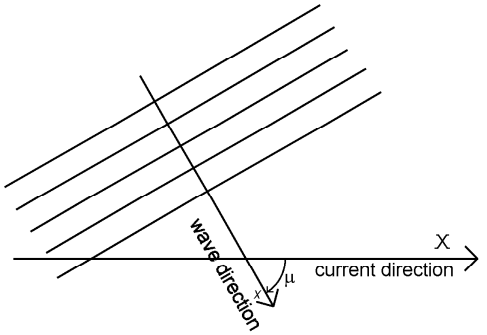

Figure 14.1: Axis System (plan view)

[0] J.M.J. Journée and W.W. Massie, *"OFFSHORE HYDROMECHANICS"*, First Edition, January 2001, Delft University of Technology. For updates see web site: http://www.shipmotions.nl.

The axis system shown in figure 5.2 in chapter 5 and here in figure 14.1 remains consistent with that used in offshore engineering:
- A current (if present) will flow in the $+X$ direction.
- The waves propagate in the $+x$ direction.
- The positive wave direction ($+x$) makes an angle μ with the X-axis.
-The $+z$-axis is upward from the still water level.

Note that this last convention, especially, can be in contrast to that used by coastal engineers (who often place the vertical coordinate origin at the sea bed). Their approach leads to numerical computational difficulties in deeper water.
The notation for some variables used in this chapter may not agree with that often used by coastal engineers; these changes have been made to make the notation within this book more consistent.

14.2 Boundary Layer under Currents and Waves

One should remember the following facts about boundary layers from basic fluid mechanics courses or the earlier chapters of this book:
- They result from a velocity difference between the ambient flow and an object.
- They need time - or equivalently distance - to develop.
- Surface roughness plays an important role in their development.

The second of these items is more obvious if one remembers that distance is an integration of velocity with respect to time.
What currents are important for this analysis? Tidal currents are driven by the gravitational attraction of the sun and the moon. These attraction forces act essentially uniformly over the entire depth of the sea, irrespective of the water depth at the given location. (This is in sharp contrast to the situation with large scale oceanographic currents - which are generally less than a kilometer deep - and the water motion caused by wind waves - which are even more 'surface-bound'.) Since the tidal current driving force is uniformly distributed over the depth, one would expect that this current would also be uniformly distributed, too. This is not the case, however - at least not in the vicinity of the sea bed. Here, the current is influenced by a friction force resulting from the water motion over the sea bed. The Prandtl-Von Kármán logarithmic velocity distribution shown in figure 14.2 results in this case. Such a velocity distribution has its maximum at the sea surface and the velocity reduces very slowly at first, but more and more rapidly as one gets nearer - in the profile - to the sea bed. The exact shape of the profile depends upon the bed roughness.
Since the logarithm of small numbers is negative, the logarithmic velocity distribution yields - strictly speaking - negative velocities in the immediate vicinity of the sea bed; this is obviously unrealistic. This shortcoming is 'patched' by using a linear (straight line) velocity profile in the area nearest to the sea bed. This line has a velocity of zero at the sea bed, and is tangent to the curve of the logarithmic velocity profile. The velocity at this elevation of tangency is often referred to as V_t. Obviously, this linear velocity profile has a constant slope, $\frac{dV}{dz}$; if the elevation of the tangency, z_t, is known and fixed, then $\frac{dV}{dz}$ is simply proportional to V_t.
The sea bed roughness (a length), which determines the details of the velocity profile can be defined in either of two ways:

- If the sea bed is essentially flat, the roughness is defined in terms of the grain size of the sea bed material.

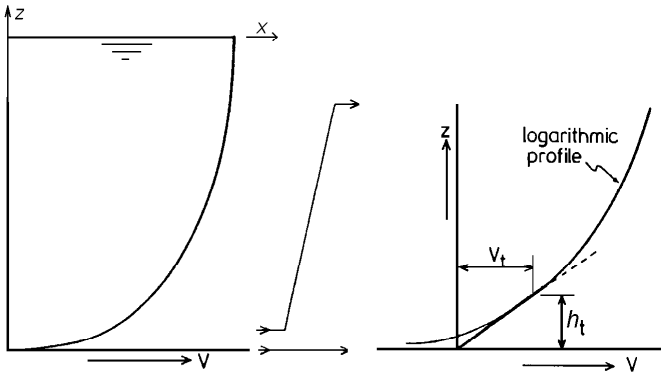

Figure 14.2: Logarithmic Velocity Distribution

- Sandy sea beds especially, are often covered with small ripples which are perhaps a centimeter or so high - much larger than a sand grain, in any case. The height of these ripples then determines the bed roughness. Such ripples are often found on the sea bed where ocean waves are present.

In both cases, the height z_t is usually of the same order of magnitude as this roughness, by the way.

14.2.1 Bed Shear Stress With Currents Alone

Newton postulated a friction model for two plates separated by a fluid - see chapter 4. It resulted in a shear stress - to use the notation of this chapter:

$$\tau = \eta \cdot \frac{dV}{dz} \tag{14.1}$$

in which:

τ	=	shear stress at bed (N/m^2)
η	=	dynamic viscosity (kg/m/s)
dV/dz	=	velocity gradient near bed (1/s)

Since the time scale in which a tidal current varies is so long, it can be treated as a constant current for the purposes of this chapter; it flows long enough for a well-developed boundary layer to develop. This means that the shear stress, τ, (caused now by the current) will also be essentially constant with respect to a time interval of several minutes or perhaps even an hour.
Constant current shear stresses also occur in rivers. If one considers a unit length (and width) of a river section, one finds that the energy input or driving force for the flow comes from the decrease in elevation (potential energy loss) over that length; the flow resistance comes from the shear stress between the river bed and flow. This yields, in an equation form:

$$\tau = \rho\ g\ h\ i \tag{14.2}$$

in which:

τ = bed shear stress (N/m^2)
ρ = mass density of water (kg/m^3)
g = acceleration of gravity (m/s^2)
h = water depth (m)
i = river surface slope dz/dx in the direction of flow (-)

In the eighteenth century, the French hydraulic engineer, Antoine Chézy, developed an empirical relationship for the depth-averaged velocity in a river. The earliest know record of its publication is 1775. It is quite certainly the first uniform flow formula for open channels; it is still used today. It is a formula:

$$V = C\sqrt{h\ i} \tag{14.3}$$

in which C is an empirical coefficient which is *not dimensionless;* it has units of $m^{1/2}/s$. It also has an inverse relation to the bed roughness: the rougher the bed, the lower the value of C.
It can be convenient to combine equations 14.2 and 14.3. Since there is essentially no constant water surface slope offshore, one simply eliminates the slope term, i, from the above two equations. This yields:

$$\tau = \rho\ g\ \frac{V^2}{C^2} \tag{14.4}$$

Notice that the water depth falls out of this equation, too, but C must still be estimated. This can be done for a constant current (at least) using:

$$C = 18\ \log\frac{12\ h}{r} \tag{14.5}$$

in which:
C = Chézy Coefficient ($m^{\frac{1}{2}}/s$)
h = water depth (m)
r = bed roughness (m)

All of this brings up an interesting question: Since V_t - the current velocity at the elevation of the point of tangency - is directly proportional to the average velocity, V, how does one explain that Newton's approach relates τ to V, while at the same time, Chézy (see [Herschel, 1897]) relates τ to V^2? One of these must be wrong, or there may be another explanation.
One is not sure that C (or even η for that matter) remains constant for a wide variety of flow conditions. Indeed, every river engineer knows that C is *not* constant. In practice, there is generally more faith in Chézy than in Newton in this case, however, so that τ is usually associated with a higher power of V or dV/dz.
The shear stress, τ, discussed so far has been the shear stress which the sea bed exerts on the flow. Newton's Third Law of motion indicates, however, that this is also the shear stress which the flow exerts on the sea bed.
Before proceeding with this development, the discussion backtracks to discuss the boundary layer and shear stress under waves.

14.2.2 Boundary Layer Under Waves

Wind waves are generally present at sea, but our river engineering colleagues did not need to consider them when they came up with their velocity profile and bed shear stress expressions. Potential theory - which by definition considers no friction - predicts that the horizontal water motion velocity caused by surface waves decreases in some negative exponential way as one proceeds deeper in the sea; see chapter 5. It is sometimes a misnomer to assume that the water motion had completely died out at the sea bed; a storm wave of 30 meters height and a period of 20 seconds still has a horizontal water motion velocity amplitude of $0,23$ m/s at the bottom - in this case in 300 meters of water! Even with more modest waves in shallower water, one can expect to have a wave-caused water motion near the bed which cannot be neglected.
Since there is a motion of the water relative to the sea bed, one might expect a boundary layer to be present. This motion is only the first of the three necessary conditions for a boundary layer stipulated above, however. One can reasonably expect bed roughness to be present, too; the third requirement is satisfied. Concern centers on the second requirement: That there is enough time (or distance) for the boundary layer to develop. Indeed, the flow in the example wave reverses every 10 seconds. There is no hope that a well-developed boundary layer can be built up. Instead, a boundary layer of very limited thickness develops in the immediate vicinity of the sea bed; the flow above this layer remains 'ignorant' of the fact that the bottom (with its roughness) is present. This neglects the diffusion of turbulence originating at the sea bed.
Analogous to the treatment of the lowest part of logarithmic velocity profile, it is convenient to assume that this wave boundary layer also will have a linear velocity profile. Continuing the analogy, this means as well that the linear velocity gradient can be characterized by a velocity at some chosen, known elevation above the sea bed; it is convenient to choose the elevation z_t for this, too. (One assumes that the boundary layer under the waves will be at least this thick; this is safe in practice.) Since the boundary layer retards the flow, it is logical that the characteristic velocity for this shear stress determination will be less than that predicted from wave theory. One generally assumes that:

$$u_t = p \cdot u_b \tag{14.6}$$

in which:

u_b = sea bed water velocity predicted by wave potential theory (m/s)
u_t = characteristic water velocity for shear stress computations (m/s)
p = dimensionless constant with a value between zero and one (-)

The above relationship is true for all times during the wave period, but it is most often used with velocity amplitudes.

14.2.3 Shear Stress Under Waves Alone

The characteristic velocity for waves, u_t, can be used in place of V_t in a shear stress relation just as was done for constant currents. One should now, however, be aware that since u_t is a periodic function with zero mean (at least to a first order approximation), the resultant shear stress - when averaged over at least a wave period - will now be zero; there is no time-averaged resultant shear stress, even though it has non-zero instantaneous values. The importance of this will become obvious later.

14.2.4 Shear Stress Under Waves Plus Currents

To combine the influences of waves and current a way must be found to combine the influences of the two boundary layers considered separately above. This is done via a careful superposition. Note that at an offshore location, the wave can propagate in any direction, μ, relative to the (tidal) current. (This is in contrast to the Coastal Engineering situation where the waves are usually nearly perpendicular to ($\mu \approx 90°$) the current direction.)
Because the sea bed portions of each of the velocity profiles - one caused by the current and one caused by the waves - are linear, the resulting profile can be expected to be linear in the near-bed zone as well. Since the current boundary layer was characterized by a velocity V_t acting at the elevation of the tangency point, it can be convenient to choose this same elevation for the wave boundary layer as well. Figure 14.3 shows a plan view (one is looking down from above) of the velocity vectors at elevation z_t above the bed.

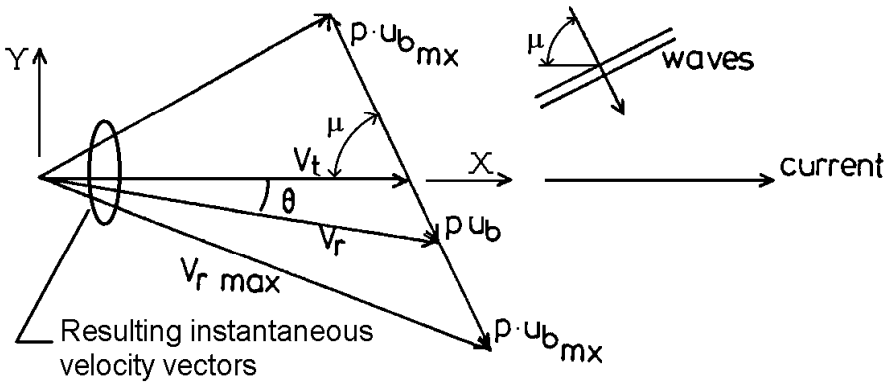

Figure 14.3: Plan View of Flow Components Just Above the Sea Bed

In this figure, V_t has been normalized to 1 m/s. The wave velocity vector has an amplitude of 0.5 m/s and makes an angle, μ, of a bit over 60° with the X-axis which coincides with the constant current velocity vector. The currents are added as vectors in this figure. The resultant velocity vector sweeps back and forth a bit in direction from one side of the axis to the other. Its magnitude changes continually, too, from a maximum of 1.30 m/s to a minimum of 0.90 m/s in this case.
The instantaneous shear stress will be proportional to the square of the instantaneous velocity and its direction will correspond to that of the instantaneous velocity. (See figure 14.4.)
This shear stress can be worked out a bit as follows.
The X and Y components of the wave current velocity will be of the form:

$$\begin{aligned} u_X(t) &= u_a \sin(\omega t) \cdot \cos\mu \\ u_Y(t) &= u_a \sin(\omega t) \cdot \sin\mu \end{aligned} \tag{14.7}$$

The constant current velocity, V_t (acting along the X-axis) will be added to $u_X(t)$.
The resulting bed shear stress magnitude at any instant is proportional to the square of this resultant velocity so that:

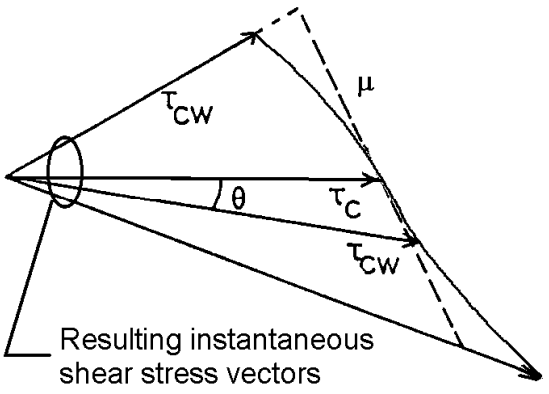

Figure 14.4: Instantaneous Shear Stresses Under Waves Plus Currents

$$\begin{aligned} |V_r^2| &= (V_t + u_X(t))^2 + (u_Y(t))^2 \\ &= \left(V_t^2 + 2\ V_t \cdot u_a \sin(\omega t) \cdot \cos\mu + u_a^2 \sin^2(\omega t) \cdot \cos^2\mu\right) \quad (14.8) \\ &\quad + u_a^2 \sin^2(\omega t) \cdot \sin^2\mu \quad (14.9) \end{aligned}$$

The instantaneous magnitude of the resulting shear stress, τ, is directly proportional to this.

Time Averaged Shear Stress Magnitude

The magnitude of τ can be averaged over a wave period as well so that:

$$\tau_{cw} = \overline{|\tau|} \quad \alpha \quad V_t^2 + 0 + \frac{1}{2}\ u_a^2 \cdot \cos^2\mu + \frac{1}{2}\ u_a^2 \cdot \sin^2\mu \qquad (14.10)$$

Noting that: $\cos^2\mu + \sin^2\mu = 1$, one comes to the final conclusion that:

$$\tau_{cw} = \overline{|\tau|} \quad \alpha \quad V_t^2 + \frac{1}{2}\ u_a^2 \qquad (14.11)$$

which happens to be completely independent of μ ! In these equations (with all velocities at height $z = z_t$):

τ_{cw}	=	time averaged bed shear stress (N/m^2)
V_t	=	current velocity (m/s)
u_a	=	amplitude of the wave motion (includes the factor, p) (m/s)
μ	=	angle between the wave propagation and current directions (rad)

This average magnitude of the bed shear stress (independent of its direction) will be found later to be important for the determination of sediment transport. Equation 14.11 makes very clear that both the current and the waves contribute to the bed shear stress; waves, if present, generally increase the average bed shear stress - in spite of the fact that the average shear stress under the waves alone is identically zero as indicated earlier in this chapter.

Time Averaged Shear Stress Components

Applying Newton's third law again, the current reacts to the time averages of the X and Y components of instantaneous shear stress. The corresponding flow velocity components responsible for each shear stress component are proportional to:

$$|V_{rX}^2(t)| = (V_t + u_X(t))^2 \tag{14.12}$$

$$|V_{rY}^2(t)| = u_a^2 \sin^2(\omega t) \cdot \sin^2 \mu \tag{14.13}$$

in which the subscript r denotes resultant.
It has been assumed in equation 14.12 that $V_t > u_X$ to guarantee that V_{rX}^2 is never negative. With this knowledge, then the time averaged shear stress in the X direction becomes:

$$\overline{\tau_x} \; \alpha \; \left(V_t^2 + 0 + \frac{1}{2} u_a^2 \; \cos^2 \mu \right) \tag{14.14}$$

This indicates that the average bed shear stress in the direction of the current is increased unless $\mu = \pi/2$.
The average shear stress in the Y direction is even more interesting. It is proportional to the time average of $V_{rY} \; |V_{rY}|$ since τ is always in the direction of the current. The result is, then:

$$\overline{\tau_y} = \frac{1}{2} \; u_a^2 \sin^2 \mu \tag{14.15}$$

which is zero only when $\mu = \pi/2$. This means that if $\mu \neq \pi/2$, $\overline{\tau_y} \neq 0$, and the resultant bed shear stress is not co-linear with the constant current. This implies in turn that there will be a resultant force acting on the water flow which is perpendicular to the original constant current direction. This force tends to divert the current so that μ does approach $\pi/2$; the current tries to turn to become parallel with the wave crests.
On the one hand, this shift in the current direction can actually take place more easily offshore than it can near the coast where other boundary conditions such as the impermeability of the beach itself also contribute to the current's behavior. On the other hand, these boundary conditions have a much smaller influence on the currents offshore; these currents tend to be stronger in deeper water and the wave influence near the bed is less than it would be in shallower water, too.

This concludes our discussion of how the sea bed influences the flow - at least for now. Results from above will be utilized in later steps, however. For now,the next step is to look at the bed shear stress in the opposite sense - to examine how the bed shear stress affects the sea bed itself.

14.3 Bed Material Stability

This section discusses the forces on and stability of cohesionless grains of bed material.

14.3.1 Force Balance

The limit of stability of (cohesionless) bed material grains can be studied via a detailed examination by an equilibrium of horizontal forces: A tiny wake - with low pressure - forms just downstream of a soil grain on the bed surface; this yields a miniature drag force, F_D, as indicated in figure 14.5.

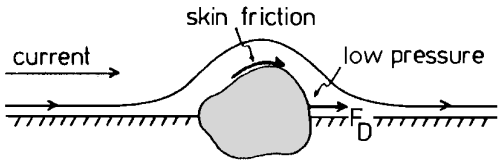

Figure 14.5: Sea Bed Grain with Drag Force

This is resisted by a horizontal inter-granular friction force which is dependent in turn on the vertical intergranular normal force. This latter force depends upon the net submerged weight (weight minus buoyant force) of the grain and the vertical resultant of the hydrodynamic pressure force distribution around that grain; see figure 14.6. (The working of this latter under-pressure or lift has been described in chapters 3 and 4. It will come up as well when pipelines are discussed in a later section of this chapter.)

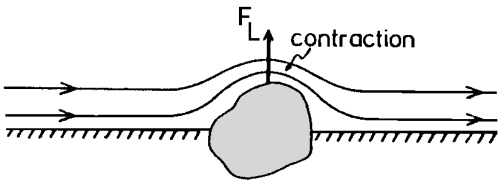

Figure 14.6: Sea Bed Grain with Lift Force

The total force 'picture' is shown in figure 14.7.

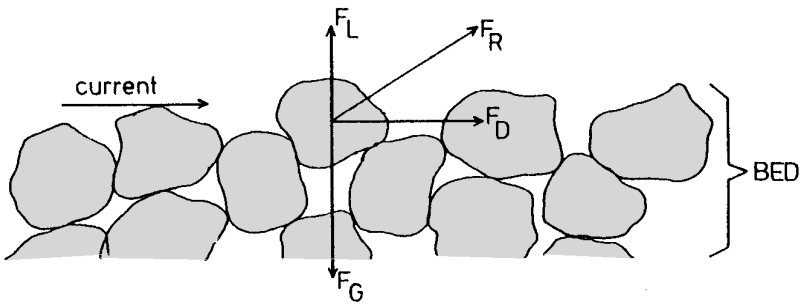

Figure 14.7: Schematic of Forces on A Sea Bed Surface Grain

One can see from figure 14.7 that a complete force balance - including the quite irregular intergranular forces - would be cumbersome to carry out at best. An alternative more global approach is therefore used instead.

14.3.2 Shields Shear Stress Approach

This alternative approach simply relates the time-average bed shear stress, $\bar{\tau}$ or τ_{cw}, to a stability parameter for the soil grains. This was first done by [Shields, 1936] for rivers. He (as well as most others!) assumed that the river bed was so nearly horizontal that its slope had no effect on the stability of the bed grains.

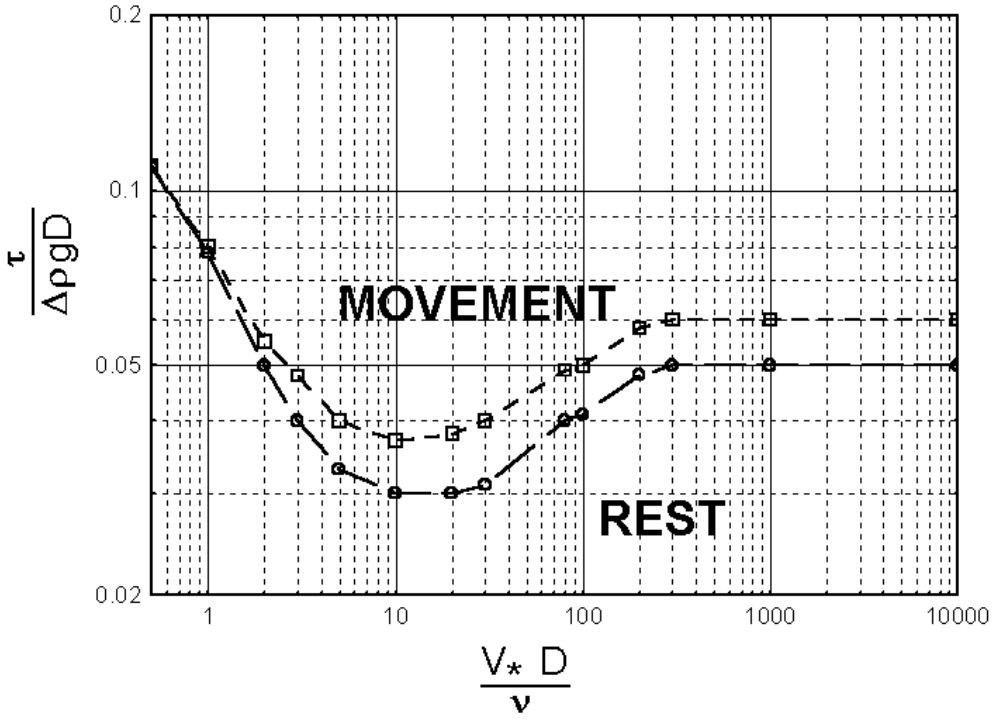

Figure 14.8: Shields Grain Stability Curve

Figure 14.8 shows the Shields relationship. The dimensionless bed shear stress,

$$\frac{\tau}{\Delta\rho \cdot g \cdot D} \tag{14.16}$$

is plotted along the logarithmic vertical axis; a grain Reynolds number,

$$\frac{V_* \cdot D}{\nu} \tag{14.17}$$

is plotted horizontally - again with a logarithmic scale.
In this figure and these formulas:

g	=	acceleration of gravity (m/s^2)
τ	=	bed shear stress (N/m^2)
$\Delta\rho$	=	$\rho_s - \rho_w$ is density difference (kg/m^3)
ρ_s	=	mass density of bed grains (kg/m^3)
ρ_w	=	mass density of (sea) water (kg/m^3)
D	=	diameter of the bed grains (m)
V_*	=	$V\sqrt{g}/C$ is the so-called shear velocity (m/s)
C	=	Chézy coefficient (m$^{1/2}$/s)
V	=	depth-averaged flow velocity (m/s)
ν	=	kinematic viscosity of (sea) water (m^2/s)

The zone between the two curves in figure 14.8 is the area of uncertainty between stability below the band, and movement above. The fact that this boundary is a bit unclear, stems from the fact that bed particles can interlock, etc., to some extent.

14.3.3 Link to Sediment Transport

One should be careful to note that bed material instability in a Shields sense is not sufficient for material actually to be transported; instability simply indicates that the particle 'cannot sit still'. Two criteria must be met simultaneously for there to be net bed material transport:

- Particles must be loosened from the sea bed; this is indicated by the Shields criterion, and
- There must be a resultant current to provide a net transport of those particles.

Since a wave, alone, provides no net current or mass transport, it fails to satisfy this latter criterion; it can only cause particles to 'cha-cha' back and forth. On the other hand, if the waves are intense enough to 'stir up' the sea bed material, then only a very small resultant current superposed on the waves can cause a very significant bed material transport. Note that this is true even when the current - if acting alone without the waves - would be too weak to cause sea bed particle instability and thus transport.

14.4 Sediment Transport Process

Now that the stability of bed material grains has been discussed, attention switches to the mechanisms by which such material is transported.

14.4.1 Time and Distance Scales

The work to be described here was first carried out for rivers. It was generally assumed that the flow conditions were not changing rapidly; a quasi-static or steady state solution was found. This means then, that accelerations could be neglected and that conditions remained essentially constant along a streamline. [Rijn, 1990] indicates that steady state conditions - in terms of sediment transport - are restored within about 80 to 100 water depths downstream from a major disturbance - such as a dam - in a river. With a typical river depth of 5 meters, this means that conditions become stable after about half a kilometer. In other words, there is still a lot of river left (usually) in which a sediment transport predicted by a steady state solution can be utilized.

For offshore conditions - in water ten times as deep, for example - this distance to regain sediment transport equilibrium becomes 5 km - a distance which far exceeds the dimensions of most offshore structures! This means that a completely stable sediment transport condition will never be achieved near an offshore structure as a result of its (local!) disturbance. Offshore engineers are continually confronted by the transient situation; this is in contrast to the situation for coastal or river engineers. Even so, it is convenient for the explanation to start with the stable or steady state situation - at least for now; the transient will be picked up in a later section.

14.4.2 Mechanisms

How is bed material transported in a river? In principle there are three ways in which it can be moved:
- solution,
- suspension and
- moving along the bed - sometimes called saltation.

Most minerals which make up the earth dissolve slowly in water and come out of solution slowly, too. Transport via **solution** is of a molecular nature throughout the water; it is not at all important for cases being considered here.
Particles in **suspension** tend to be relatively fine; they move along with the water which surrounds them. This transport can take place at any elevation in the flow. It is suspended transport which often makes water look turbid or 'hard to see through'.
Saltation, or **bed load transport** 'never really gets off the ground' - to put it popularly; it rolls and bounces along the bed with a speed which is less than that of the adjacent flow in the sea bed boundary layer.
These latter two transports are discussed a bit more below.

Suspended Transport

It will later become obvious that suspended transport is only occasionally important for offshore engineering applications. The following discussion is given for completeness and to provide a basis of understanding for some other phenomena.

What mechanism keeps bed materials in suspension? Suspended sediment particles fall back toward the sea bed with their fall velocity. (This was discussed in chapter 4.) Material is moved back upward as a result of turbulent diffusion and the fact that the water exchanged upward has a higher sediment concentration than the water swapped downward at the same time. This is illustrated in figure 14.9.
Further, there is usually a free exchange of material between the flow and the sea bed. Generally, no suspended material is lost at the sea surface. This can all be put together to yield a classical ordinary differential equation for an equilibrium situation:

$$V_f \; c(z) + \epsilon(z) \, \frac{dc(z)}{dz} = 0 \tag{14.18}$$

in which:

V_f = particle fall velocity in water (m/s)
$c(z)$ = sediment concentration at elevation z
$\epsilon(z)$ = turbulent eddy viscosity at elevation z

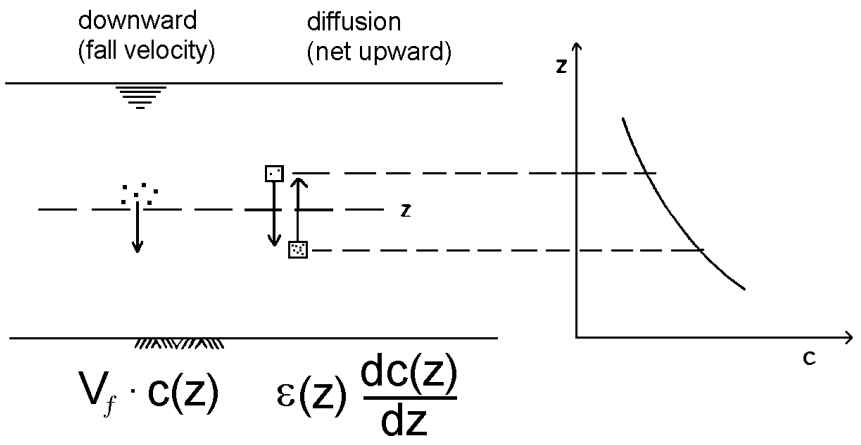

Figure 14.9: Vertical Suspended Sediment Transport Balance

ϵ is a measure of the scale of turbulence in the flow. By assuming a distribution for $\epsilon_s(z)$, one can work out the solution to equation 14.18. After a bit of mathematical manipulation (which is not really important for our insight here) the coastal engineers get a solution which looks like:

$$c(z) = c_a \cdot \left(\frac{-z}{z+h} \cdot \frac{a}{h-a} \right)^{z^*} \tag{14.19}$$

in which:

$c(z)$	=	sediment concentration at elevation z
c_a	=	sediment concentration at a chosen elevation $a > 0$ above the bed
h	=	water depth (m)
z	=	vertical coordinate, + upward from the water surface (m)
z^*	=	dimensionless parameter (-), dependent upon τ, ρ and V_f (The exact background of z* is not important here)
V_f	=	the particle fall velocity (m/s)

The sediment concentration at some chosen elevation, a, must be known in order to determine the quantitative solution of equation 14.19. One will discover below that this comes from the bed transport to be discussed in the next section.
Once $c(z)$ is known, the total rate of suspended material transport follows directly from the following integral:

$$S_s = \int_{bed}^{sea\ surface} U(z,t) \cdot c(z) \cdot dz \tag{14.20}$$

in which:

S_s	=	suspended sediment transport (m^3/s per meter width)
$U(z,t)$	=	velocity (from any cause) at elevation z and time t (m/s)

This is usually simplified a bit if waves are involved; one is not interested in a truly instantaneous sediment transport. Its time average (over a wave period) is much more relevant. This allows $U(z,t)$ to be replaced in 14.20 by its time averaged value, $\bar{U}(z)$.

Bed Load Transport

Bed load transport 'never gets off the ground'; it stays near the bed in a thin layer below the suspended sediment transport. The same forces which determine particle stability also govern bed load transport. In contrast to the situation with suspended transport, the bed load moves more slowly than the water near the bed; most formulas for predicting the rate of bed load transport, S_b, express this rate directly instead of via a concentration times a velocity as was done with suspended transport. Indeed, the water velocity is changing rapidly as a function of elevation here and the sediment concentration is hard to define in this region, too.
On the other hand, a sediment concentration - at some elevation - is needed in order to determine the actual suspended sediment concentration profile as explained above. It is convenient to perform this coupling near the sea bed - more specifically at an elevation h_t above the bed - the height at which the linear near-bed velocity profile is tangent to the logarithmic Prandtl-Von Kármán profile. It is being assumed (quite arbitrarily) that transport above this level takes place in suspension and that only bed load transport is found below.
Hydraulic engineers have taken the very pragmatic step of converting the bed load transport into a (form of) concentration by assuming that S_b takes place in a layer of thickness h_t and with a velocity equal to V_t. This equivalent 'concentration' is then:

$$c_a = \frac{S_b}{h_t \cdot V_t} \tag{14.21}$$

Using this link, one can relate the entire steady state sediment transport, $S = S_b + S_s$, to one quantity: The bed transport, S_b. Attention can be concentrated on determining this value. Before doing so, however, the relative importance of S_b and S_s for offshore applications will be examined in this next section.

14.4.3 Relative Importance of Bed versus Suspended Load

Many comparisons can be included under this heading. River engineers are often interested in the ratio of suspended load transport to bed load transport, S_s/S_b. This value can vary widely in rivers, by the way; it can be high (thousands) for a muddy river such as the Amazon or Mississippi, and very low ($\ll 1$) for a sparkling clear mountain stream tumbling over rocks.

In offshore engineering on the other hand, one is wise to first consider the relative time (or distance) scales within which S_b or S_s change. Consider what happens to each of these quantities when - for example - the near-bed flow is locally disturbed by a partially exposed submarine pipeline, for example. Such a pipeline will typically be no more than a meter in diameter and it may protrude 50 centimeters or so above the sea bed. At the same time, the water depth can easily be in the order of 100 meters.
Using potential theory from chapter 3 to estimate the order of magnitude of the disturbance caused by the half-buried pipe, one finds that at a distance of at little as 1 meter above the sea bed (above the pipe) the velocity has only been increased by 25%. At 2 meters height this increase is only a bit more than 6%. The conclusion must be that the pipe only disturbs the velocity field in its immediate vicinity. Consequently, the velocity gradients and thus the local bed shear stresses and vertical diffusion of sediment will be disturbed only locally as well.

One can expect the bed transport, S_b, to react quickly to these changes. Indeed, each bed transport particle can stop any time it hits the bottom and this happens almost continuously. The bed transport can adjust or adapt itself several times within a distance of a few meters.
The material making up the suspended transport, S_s, on the other hand, does not frequently come in contact with the bottom; it gets little opportunity to stop. Except that flow in the immediate vicinity of the pipe - especially in its wake - may be a bit more turbulent, the rest of the (tidal current) flow does not even 'notice' that the pipe is there; the major part of the flow as well as the suspended transport it carries is essentially undisturbed by such small scale changes.

Some may argue that whenever S_b changes, S_s will change as well. Their reasoning follows from the link established above between suspended and bed load transports. What they fail to realize is that this theoretical 'link' was established for an equilibrium situation and that a change in S_s must take place via changes in its sediment concentration profile. The driving forces for determining that profile - the turbulent diffusion and the particle fall velocity - are not (or only very locally) changed. It is indeed because of S_s that [Rijn, 1990] concluded that a distance of 80 to 100 water depths is needed for an equilibrium sediment transport to be reached in a river.

The conclusion to all this is that bed load transport reacts very quickly to flow changes which occur on a scale typical of offshore engineering objects, but that suspended transport does not. Offshore engineers seldom have to worry about the transport of suspended material. S_b is almost always the most important transport component in an offshore situation. Conversely, S_s is seldom important in an offshore situation!

14.5 Sea Bed Changes

14.5.1 Sediment Transport Not Sufficient for Bed Changes

Having bed material instability (in the Shields sense) and having a resulting current to transport that material is not usually sufficient to cause a real morphological problem (erosion or deposition). The presence of sediment transport past a point only indicates that the bed material grains now present at that location will (probably) be replaced by others within a very short time; a dynamic equilibrium can exist.
In order to have (or reveal) morphological changes as a result of sediment transport, one must examine dS/dX, the change in sediment transport along a (resulting) streamline. If S increases as the flow proceeds from point A to point B, as shown in schematic cross section in figure 14.10, then the extra material transported past point B (if dS/dX is positive) can only have come from the bed segment between A and B; a positive value of dS/dX leads to erosion. Conversely, a negative value must lead to sedimentation or deposition of material in the segment between A and B.
How does a time dependence affect the situation? When the current changes slowly as a function of time - such as with a tidal current - this makes no difference. This variation only introduces a dS/dt which is pretty much the same in the entire vicinity; this does not - of itself - yield either a significant erosion or deposition.

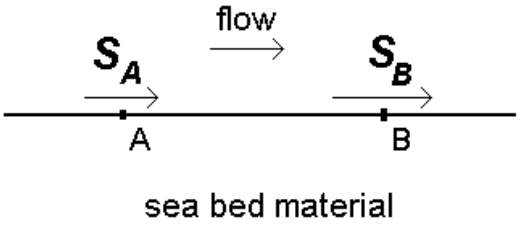

Figure 14.10: Longitudinal Bed Section Along Flow Line

14.5.2 Bed Change Time Scale

Coastal engineers work on a large scale. They are typically concerned with a beach which can be hundreds of meters wide and many kilometers long. Hundreds or even thousands of cubic meters of bed material must be removed or deposited in order to make a significant impact. This can take so long that the beach never really 'comes to rest'; it keeps on changing continuously. Because of this, coastal engineers invest a major portion of their efforts in determining the speed with which (coastal) conditions change. They need to predict how much a given coastline will change in - for example - the coming decade as a result of natural accretion and erosion resulting from waves and currents along the coast.

Typical objects for which sea bed morphology is important to offshore engineers include a pipeline, the base of a jack-up platform leg or even an entire steel tower structure. Smaller objects can include equipment lost overboard, an anchor or a communications cable. Offshore engineering morphological phenomena take place within a distance of no more than some tens of meters. As a consequence of this, only a relatively very small amount - very often less than a hundred cubic meters - of bed material needs to be removed (or deposited) in order to reach a new equilibrium. One can intuitively feel (correctly) that this can occur much faster. Indeed, morphological changes significant for offshore engineering often occur during a single tide period - usually when there is a storm going on. This enhances the wave action and thus the magnitude of the bed shear stress. This in turn stirs additional bed material loose from the sea bottom so that the resulting current - locally influenced by the pipeline or other object present - can transport it.

14.6 Laboratory Modeling

Before discussing applications, our attention will be temporarily diverted to the topic of physical modeling of local morphological changes.

14.6.1 Theoretical Background and Scaling

Imagine the physical problem of modeling the morphology of a the area around a pipeline in say 100 meters of water. Since waves are involved, one uses Froude scaling; see chapter 4 or appendix B. If the wave and current flume has a maximum depth of 1 meter, one would be forced to use a geometric scale of 1 : 100. At this scale, a cylinder with a diameter comparable to that of a pencil would be a reasonable pipeline model. This is too small; The Reynolds number, etc. become too distorted.

A more inspired physical model is possible, however. Since offshore morphological problems are dominated by bed load transport, there is no real need to model the suspended transport correctly - or even at all for that matter. Since the bed load moves along in a thin layer near the bed, why, then, is it necessary to model the entire ocean depth? Indeed, this is no longer necessary at all!
With this knowledge, one can modify the laboratory model so that only some meters (in height) of the near-bed flow is reproduced as is shown in figure 14.11.

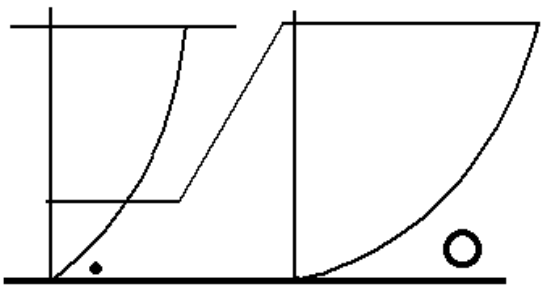

Figure 14.11: Schematic Longitudinal Section of Field and Model Conditions

The height chosen must be such that the pipeline - which is now larger, too - does not significantly 'block' the entire flow; this would introduce extra influences not found in nature. A good rule of thumb is that the object being studied should not block more than 1/10 (or 1/6 at the very worst!) of the flow cross section. With this, an exposed model pipeline about 80 mm in diameter would require a water depth of about 800 mm, leaving a freeboard in the flume of 200 mm for waves or any other disturbances.
It should be realized as well, that this model no longer represents the entire flow depth; it only includes the lower meters of the prototype situation. What is the consequence of this? What current velocity should now be used in the (new) model? It is no longer correct just to scale the depth-averaged velocity from the prototype for use in the model. Instead, the depth average of the current in the (lower) portion of the velocity profile - the part actually being modeled - should be reproduced (to an appropriate scale, of course); this has already been suggested in figure 14.11.
What about waves, then, one can ask? The surface waves from the field will be much too near the sea bed in the 'cut down' model! Here again, it is the velocities near the bed caused by the waves that must be reproduced to scale.
Since it will be generally necessary to reproduce the spatial effects - in the horizontal direction - it will be necessary to scale the wave length according to the geometric scale; this - with the water depth - sets the wave period relationship in accordance with Froude scaling. One obtains the proper bed velocity amplitude by adjusting the wave height; this compensates for the fact that the water depth is not scaled in the same way as the rest of the model.
One would probably not choose the actual current velocity to be used until this step was completed by the way - in spite of the discussion above! One (alternate?) approach is to scale the current velocity using the same ratio as was found for the wave motion velocities.
The key to successful physical modeling of sea bed sediment transport is to properly scale the bed shear stresses in relation to the stability (in the Shields sense) of the bed material. This fact may require that both water motion components be adjusted to achieve the

proper match of the sea bed flow conditions to the stability of the bed material used in the model. Indeed - to complicate matters even more - one may be using a different bed material in the model than one finds in the field.

14.6.2 A Modeling Experience

This relates to a modeling situation actually encountered by a thesis student in the mid nineties. He was conducting lab experiments to check the stability of stone berms occasionally used to cover otherwise exposed subsea pipelines. The tests were being carried out in a wave and current flume with wave propagation in the same direction as the current.
On the fateful day, a berm of loose stone had been built across the bottom of the flume; it had a slope of 1 : 5 on both the upstream and downstream sides; the crest height was such that the water depth on top of the berm was about 90% of that in the rest of the flume. This was in accordance with all the criteria stated above. Figure 14.12 shows a (distorted) cross-section of the berm and thus also a longitudinal profile of part of the flume. The water surface is well above the top of the figure and only the surface layer of berm gravel is represented in the sketch.

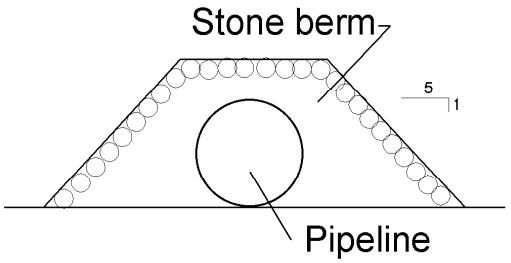

Figure 14.12: Longitudinal Section of Berm Model

As a check, the first tests of the day were carried out with just a current. After the current had been increased in a few steps, the bed shear stress on the crest of the berm became high enough to cause instability of the stones; quite a rapid erosion started - with the stones being deposited downstream at the toe of the berm.
Remembering from the theory that waves, if present, increase the bed shear stress and thus the sediment transport rate, the student hastened to start the wave generator in order to be able to observe a really spectacular erosion process. Can you imagine his dismay when - after the waves had been added - the stones in the berm remained stable! What was wrong with the experiment? Is the theory wrong?
After recovering from the initial shock, he investigated the matter systematically as follows: The distorted berm profile was fixed in place (by sprinkling fine cement into its pores and letting it set) and a series of local velocity profiles were measured at various locations around the berm using a laser anemometer. Since bed load sediment transport is governed by the bed shear stress, the laser beams were set close to the berm surface to make measurements in the boundary layer in order to determine the velocity gradients and thus infer the bed shear stresses from the local flow parameters.
Just as in the seemingly ill-fated experiments, tests were carried out both with a current alone and with waves superposed on the current. To everyone's surprise, the velocity profile

measurements revealed that the velocity gradients (and thus the shear stress on the stones) above the berm crest were greatest when just the current was present!
Apparently, when the waves were added to the current, they interacted with that current and with the berm, and possibly other parts of the flume itself, in such a way that the gradients in the velocity profiles above the berm crest were reduced instead of enhanced by the waves. This confirmed that the experiments still agreed with the basic theory; the experiment was just a bit different that had been expected!
The morals of this whole experience are that the bed shear stress is important for determining bed load sediment transport and that such experiments must be carried out very carefully. Persons trying to predict stability or erosion or deposition of bed material can best do this by evaluating - only in a qualitative way if necessary - the local bed shear stress and the changes which it undergoes as the flow progresses along the streamline.

14.7 Vertical Pile in Current

The first application involves a somewhat isolated vertical pile which penetrates well into the sea bed and protrudes above the bed to a height of at least several diameters. The discussion which follows includes both the hydrodynamics and the resulting morphology - both now in three dimensions.

14.7.1 Two Dimensional Approach

Remembering the 2-dimensional hydrodynamics (in a plan view, now) of the flow around a circular cylinder, one knows that there is a stagnation point at the most upstream side of the cylinder and a wake behind the cylinder. Also, theoretically at least, the velocity on each side immediately adjacent to the cylinder is twice that of the undisturbed ambient flow.
Since there is no velocity at a stagnation point, one would expect little to happen to the bed on the most upstream or 'leading' part of the pile; at the sides where the velocity is locally doubled, one might very reasonably expect an increased shear stress, too, yielding a positive dS/dX and thus a local erosion. The extra turbulence caused by the wake could enhance erosion on the lee side of the cylinder, too. This would leave the cylinder standing in a 'pit' (except on the upstream side).

One of the world's greatest tragedies is the murder of a beautiful theory by a brutal set of facts: One observes - in nature or even in a lab experiment - that there is a significant erosion hole on the entire upstream side of the cylinder. This extends along the sides (where it is already expected) and 'fades out' in the wake area. Apparently, the two-dimensional approach is insufficient to explain what happens.

14.7.2 Three Dimensional Flow

The three-dimensional flow pattern includes the velocity profile (in the vertical) caused by bed friction in the ambient current. Figure 14.13 shows a longitudinal vertical section with the approaching velocity profile shown on the left. The current shown here is quasi-constant such as a tidal current. Waves are not needed for this explanation; they just complicate the discussion in this case.

Consider now horizontal cross sections at two different elevations, A and B, in that figure. Because of its higher location, the approaching current at elevation A will be faster than at location B.

$$V(A) > V(B) \tag{14.22}$$

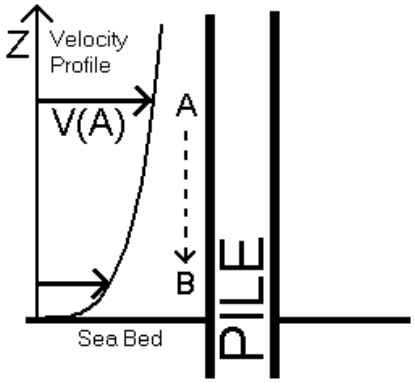

Figure 14.13: Pile with Approaching Velocity Profile

This implies, in turn, that the stagnation pressure at A, $\frac{1}{2}\ \rho\ V^2(A)$, will be greater than the stagnation pressure farther down along the pile at point B. Along the vertical line of stagnation points on the upstream side of the pile one will find a dynamic pressure gradient which is steeper than the hydrostatic gradient, $\rho\ g$; there will be a residual quasi-static downward pressure gradient along the upstream side of the pile! This pressure gradient will result in a downward flow along these stagnation points as indicated by the dashed arrow in figure 14.13. What happens to this flow when it hits the sea bed?

Horseshoe Vortex

After colliding with the bed, the flow turns upstream, along the bed against the approaching flow (where the approaching velocity is lowest) as shown very schematically in figure 14.14. This flow can turn upstream here along the bed because the kinetic energy of the

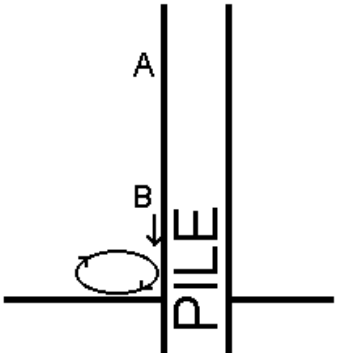

Figure 14.14: Schematic Detail of Horseshoe Vortex just Upstream from the Pile

approaching flow is low here, anyway. After progressing a short distance - think in terms

of a pile diameter - it bends up and is swept back to the cylinder to form a vortex. This vortex grows in length on each side; its ends (or tails) get swept around the cylinder by the flow so that this vortex takes on a U-shape resembling a horseshoe when viewed from above.

A common feature of vortices is that they are local and have higher flow speeds than one would otherwise expect in the vicinity. A vortex has a relatively thin boundary layer adjacent to an object or the sea bed so that relatively high velocity gradients and turbulence (in their radial direction) result. Given this - and remembering that shear stresses are dependent upon velocity gradients - it is not surprising at all that an erosion pit develops on the entire front and sides of the pile.

What prevents this erosion from going on 'forever' and making a pit of unlimited depth? After all, the horseshoe vortex is not time limited. As the erosion pit gets deeper, the slopes at its sides become steeper. This upward slope - as seen in the direction of local flow - makes it more difficult for bed material to be transported. (Remember that slopes have been neglected in sediment transport discussions.) In practice with a nice sandy bed, one can expect this erosion pit to develop to an ultimate depth of in the order of 1.5 pile diameters. All of these phenomena are illustrated in figure 14.15.

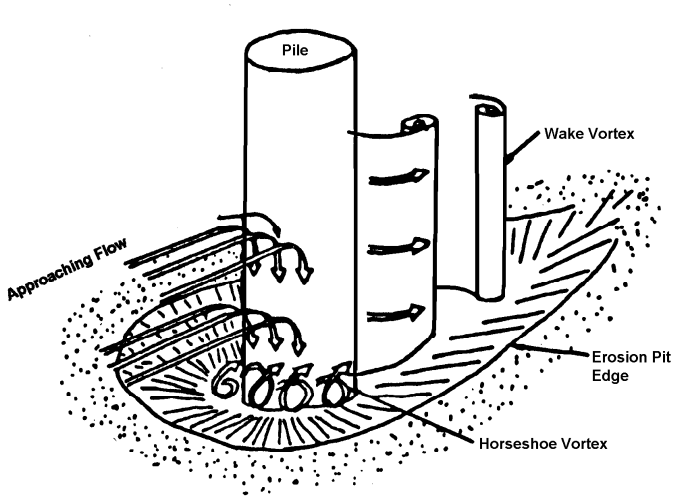

Figure 14.15: Final Overall Bed Situation Near Pile

What happens to the material eroded from the pit, and what happens on the downstream side of the pile? Here the vortices in the pile wake cause increased turbulence. Also, the story about stagnation pressures can be repeated here, but it now works in the opposite sense. A small secondary flow of water coming from the sea bed - and even from the horseshoe vortex - will be drawn upward into the wake. Is it surprising that this flow also carries sediment in suspension? Its (temporarily) increased turbulence makes this possible. However, once the flow is swept downstream past the pile, no new turbulence is added and the vortices in the wake gradually die out. The sediment that had been picked up in the immediate vicinity of the pile now falls out on a relatively extensive area downstream.

Flow Reversal

What happens when the tidal current reverses direction and - to make this discussion clearer - flows from north to south instead of from south to north? It has just been explained that the 'original' erosion pit generated by the south to north current was formed on the east, south and west sides of the pile. Now, after the current reverses, the pit will form on the east, north and west sides. The existing pit on the south side which is now in the wake will most likely fill up a bit with very loose material.

Final Erosion Pit

As a consequence of tidal action, therefore, one can expect - for design purposes - an erosion pit to be formed completely around any slender vertical pile. The depth and width of this pit will be in the order of 1.5 pile diameters. This, in turn, means that the lateral support of the pile begins only 1.5 pile diameters below the sea bed; this can have consequences for the design of the foundation (in a geotechnical sense) as well as the pile (in a structural engineering sense).
Using the above rule of thumb for a pile 2 meters in diameter as an example, one finds that roughly 50 m^3 of bed material will be removed to form the stable state erosion pit. In onshore terms, this is not even two truckloads of earth - relatively little, indeed. One can indeed expect this erosion pit to form quite rapidly - usually within a single tide period.

14.7.3 Drag Force Changes

Even though hydrodynamic forces on a pile are not of primary interest in this chapter, it is convenient to discuss drag forces on the cylinder here, too - at least to the extent that they are influenced by the velocity gradient caused by bed friction.
One will already know that the drag force acting on a vertical cylinder in a constant current of velocity, V, will be given by:

$$F_D(z) = \frac{1}{2}\,\rho\,C_D\,D\,V^2(z) \tag{14.23}$$

in which:

$F_D(z)$	=	drag force per unit length at elevation z (N/m)
ρ	=	mass density of the fluid (kg/m^3)
$V(z)$	=	approaching velocity at elevation z (m/s)
D	=	pile diameter (m)
C_D	=	cylinder drag coefficient (m)

Does $F_D(z)$ change because the velocity profile is present or because of other factors not accounted for by the strictly two-dimensional flow pattern assumed in the earlier discussion of forces in chapter 4? There are two additional effects discussed so far: One at the sea bed and one at the water surface.

Secondary Flow Effect at Sea Bed

The secondary downward flow on the upstream side of the pile leads to the horseshoe vortex formation at the bed, but it also supplies an extra volume of water which flows around

the cylinder at the bed elevation. Looked at in another way, the flow past the cylinder near the bed is actually greater than one would expect to find based upon the undisturbed approach velocity at that level.
Since the (measured) force is generally related to a velocity which in fact is smaller than one would associate with that actually present, one will find a slightly larger value for the drag coefficient, C_D. A plot of C_D versus depth will increase a few percent near the sea bed.

Water Surface Effect

The pile will cause what looks like a standing wave at the water surface. It is in fact a travelling wave which propagates upstream at a speed identical to that of the flow at that level. In this way, the wave stays synchronized with the pile location. This small wave generates a dynamic pressure field which dies out exponentially with depth (just like that of any other short wave). Since the wave crest (with higher pressure) is near the upstream part of the pile and the wave trough (with lower pressure) is on the downstream side, this wave will cause a net (additional) force component in the direction of the flow.
When the total drag force at this level (including this additional component) is related to the undisturbed near-surface flow velocity, it is only logical that the associated C_D value will be a few percent higher at this elevation.

Free End Effect

A third effect is more often encountered in the lab. One simple way to measure drag forces in a towing tank is to extend a cylinder vertically downward into a towing tank and to tow it while measuring its total resistance as a function of towing velocity. The force is then assumed to be uniformly distributed over the submerged length of the cylinder in order to ultimately arrive at a C_D value. Is this correct?
This will not be precisely correct for the following two reasons: The force will be disturbed (slightly) by the surface wave already discussed above, and there will be a three-dimensional flow pattern near the free, submerged end of the cylinder. This end effect will reduce the force there.

None of these force disturbances are significant enough for one to have to worry about them when predicting loads on an offshore structure. The situation can be quite different if one is determining a drag coefficient value from experiments in the lab, however.
These end effects - as all three of these phenomena are sometimes collectively called - can be eliminated for tests with currents only by adding thin but rigid horizontal plates to the cylinder: One just below the water surface and one near its free end. The upper plate should be larger than the wave length of the surface disturbance wave; the top of this plate will absorb the wave's dynamic pressure, thus preventing it from disturbing the pressure field lower down in the water. The lower plate will force the flow around the cylinder above it to remain two-dimensional.
Obviously, it would be best if the drag force was measured now only on some segment - located between the two guiding plates - of the total cylinder length. If this is done, however, and the measuring section is far enough from the water surface and the free end anyway, then it is not necessary to install the flow-guiding plates in the first place.

If measurements are to be made in waves, it is impossible from the start to use plates to guide the flow around anything except a cylinder submerged horizontally with its axis parallel to the wave crests.

14.8 Small Objects on The Sea Bed

There is a whole variety of small objects that can be found on or in the sea bed. In some cases the objects are intentionally deployed; anchors, subsea positioning beacons, or even mines and military listening devices fall into this category. Cargo items which fall overboard are generally not intentionally deployed on the sea bed - think of an automobile from a ferry or a small container being lifted to an offshore platform. The total list of objects one can find on the sea bed is nearly endless.
In some cases it is necessary that an object remain exposed on top of the bed; the functionality of a subsea beacon can depend upon this, for example. In other cases prompt self-burial is desired as a means of reducing the chance of detection of certain military devices. Here, again, the range of possibilities is broad.

14.8.1 Burial Mechanisms

How can an object which falls overboard become buried? There are several mechanisms conceivable:

- It can hit hard enough to create its own crater which is then re-filled by 'conventional' sediment transport. The chance that this occurs is small, however. Most objects don't fall fast enough to have enough impact energy. Indeed, as indicated in chapter 4, the fall velocity of most objects in the sea is modest. The pile dropped vertically was a striking (no pun intended) exception to this, however; see chapter 4.
- The object sinks into the soil under its own weight. This implies that there will be a soil bearing failure under the object. For this to happen, either the object will have to generate a high normal stress on the sea bed, or the bed material will have to be relatively weak - think of a very soft mud in this latter case. Such self-burial will often require a heavy and specially shaped object.
- An object can become buried as a result of local erosion and deposition. This is 'our' type of problem which will be discussed more below.
- The object may be covered or exposed as a result of large scale bed form mobility. Many of the large sand banks or shoals along the Dutch coast migrate slowly northward as a result of material being eroded on one side and re-deposited on the other.
- Sudden large scale sea bed movements can take place, triggered by very high storm waves or even by an earthquake. These can expose, cover, or even sweep away an object in their path. This has happened from time on the continental slopes. This was detected when transatlantic communication cables were suddenly broken and swept away. The time lapse between the failures of successive cables even yielded insight into the propagation speed of such slides.
- A last mechanism results from the possible slow build-up of excess pore pressure in the soil - usually an initially loosely-packed fine sand. This will be discussed below, too.

Local Morphology

The morphology near the (small) object on the sea bed has much in common with the pile. The object will generally stick up a bit but not have a nicely streamlined form. Since it is sticking up into an ambient velocity profile, it is logical that a downward secondary flow develops on the upstream side; this will result in some form of horseshoe vortex on the upstream side at the sea bed, just as near the pile. This vortex will again start creating an erosion pit immediately upstream of and beside the object as shown (as a longitudinal section) in figure 14.16.

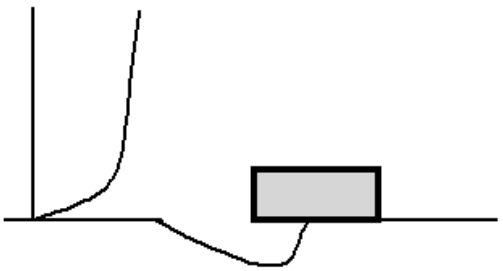

Figure 14.16: Small Object with Approaching Velocity Profile and Upstream Erosion Pit

Now, however, since the object does not penetrate significantly into the sea bed, material from under the object will fall into the pit; the object's support is eroded on the 'upstream' side, too. The result of this is often that the object ultimately tips forward into its 'own' erosion pit. Depending on the exact shape of the object, this can then change the local flow geometry significantly as well.
Such a fate is common for small irregular objects such as odd cargo items no bigger than a meter or so in maximum dimension. Short, stubby concrete cylinders - often used as inexpensive moorings for navigation buoys, etc. are another excellent example of this.

Pore Pressure Buildup and Bed Instability

Pressure changes on the surface of the sea bed which result from surface (storm) wave action can cause minute cyclic soil deformations. Loosely packed soil will 'try' to consolidate, thus reducing its void volume. Since the soil is saturated, water will have to escape during this consolidation process. Fine soils - even fine sand - can have a low permeability; this in combination with the oversupply of pore water, leads to an increase in pore pressure. Since Terzaghi's rule that:

$$\text{Total Stress} = \text{Grain (or Effective) Stress} + \text{Pore Pressure} \tag{14.24}$$

is valid, the increased pore pressure results in a reduction of effective grain stress. In the limit, a quicksand condition occurs in which the effective stress has become too small to withstand the applied loads. Such a soil then behaves more like a high density fluid instead of a solid.
If the density of an object is less than that of quicksand (in the order of 1800 kg/m^3), it will 'float' in the quicksand and move slowly and incrementally to the bed surface; a heavier item sinks, instead. Pipelines - when filled with air (just after installation) or even with gas

often have an overall density of about 1300 kg/m^3; they have been known to 'float' upward through a beach and become re-exposed. At the opposite end of the scale, electric and some communications cables buried in the ground or sea bed will have an overall density of more like 4000 kg/m^3; they will indeed sink.
Note that it is not absolutely necessary for the quicksand condition to become 'fully developed'. The soil's effective intergranular stress and thus its shear strength is reduced as soon as the pore pressure increases. Since the net vertical force exerted by the buried object - it does not matter if it is positive or negative - will also cause shear stresses in the surrounding soil, it is only necessary that the soil's shear strength be reduced below the imposed stress level for failure to occur. Actual failure usually occurs slowly, the cyclic wave action stimulates cyclic variations in the pore pressure so that the failure is intermittent rather than continuous.
Relatively large pressure cycles are needed in order to build up sufficient pore pressure for this whole process to take place; this makes it essentially a shallow water phenomenon in the marine environment. At leas one newly-installed pipeline has floated up after being buried across a beach in The Netherlands. Luckily the problem became apparent before the pipeline was put into service.
In an onshore situation, electric cables laid in poor soil have been 'lost' in that they have sunk deeper - except where they are held in place in a junction house! In this case, the vibration source was the traffic on the adjacent highway.
What can be done to prevent this problem - at least in the marine situation? There are two possible solution approaches:

1. Consolidate the sand artificially as the pipeline or cable trench is being backfilled. While this is theoretically possible, it is probably a pretty expensive solution for a pipeline - even when one can work from the beach! Hydraulic engineers have used this approach however during the construction of the dam in the mouth of the Eastern Schelde. There, they feared that vibrations of the barrier support structures could lead to pore pressure build-up and subsequent failure of the deeper sand layers.

2. Backfill the pipeline trench with coarser material, providing sufficient soil permeability to prevent pore pressure build-up. This is the most commonly chosen preventative measure - at least for offshore situations.

14.9 Pipelines

This section discusses forces on exposed pipelines as well as the sea bed morphology in their vicinity. The discussion of hydrodynamic forces on pipelines has been delayed till this point because the presence of the current velocity profile caused by bed friction plays such an important role in the hydrodynamics.
A pipeline seems like a small object when seen in cross-section; in the third dimension it is very much a one-dimensional or line-like object. Much of what was discussed about small objects on the sea bed turns out to be applicable to pipeline cross-sections as well. The reader must be careful, however; since differences do exist. The following discussion will be for a pipeline which is initially laying on the sea bed with only a minimum of penetration into that bed (caused by its own weight). The current will flow more or less perpendicular to the pipeline route. The sea bed material is sand.

14.9.1 Flow and Forces

Because the pipeline is bedded slightly in the sand, it will not allow flow to pass under it; the entire approaching flow will have to pass over the pipeline. This flow pattern is obviously quite distorted relative to that for an isolated cylinder far away from any flow-constraining walls.

Drag Force

The drag coefficient for the pipeline will be somewhat higher than that for the cylinder in the unrestricted flow. This higher drag coefficient is then used in conjunction with the undisturbed current at the elevation of the pipeline center line. Remember that there is a strong velocity profile gradient here! Continuing the discussion of the horizontal equilibrium, first, the drag force is resisted by a friction force which, in turn, depends upon the contact force between the pipeline and the sea bed; horizontal stability depends upon the vertical force balance, too. These forces are all illustrated schematically in figure 14.17. There will be something similar to a stagnation area - with an associated relatively high quasi-static pressure - on the upstream side of the pipe near the bed.

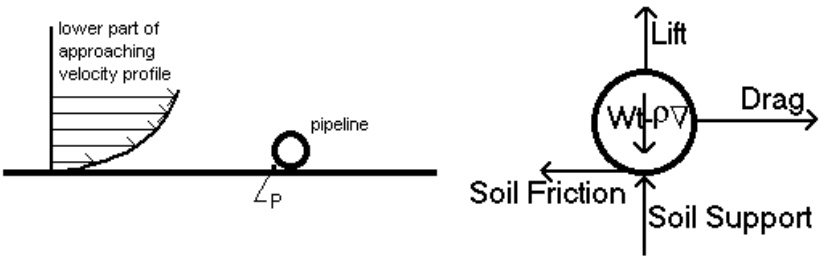

Figure 14.17: Flow Situation and Forces on a Cross Section of Exposed Pipe

Lift Force

Because of the approaching velocity profile and the fact that all of the flow must pass over the pipe, the velocities on top of the pipe will be even higher than those predicted by potential theory for an isolated cylinder. The concept of reflection was used in chapter 3 to model a potential flow around a cylinder near (or in contact with) a flat bed, but this still neglects the influence of the velocity profile in the approaching flow.
A high velocity along the top of the pipe implies low pressure there, while the water on the underside of the pipe - near point P in figure 14.17 - is nearly stagnant.
Conceptually, this begins to resemble the net flow effect of an isolated cylinder in a uniform current and surrounded by a circulation; the net force effect will be a lift directed perpendicular to the current - upward in this case. This force will have to be counteracted by pipe weight.
Looking for a moment at the total vertical equilibrium, this lift force reduces the soil contact force and thus, indirectly, the sliding friction resistance from the bed. Unless the pipe is constrained somewhere else along its length, it will slide sideways before it lifts off the bottom.

It is usually most economical to provide sufficient pipeline weight (for larger lines) by adding a high-density concrete coating; for smaller lines it can be more economical just to increase the steel wall thickness a bit. In either case, however, the added weight increases the pipe's outside diameter. One can quickly realize that as the outside diameter is increased, the drag and lift forces are increased, too! One is 'chasing one's tail' so to speak. Even so, an iterative solution can be found so that a stable design can be achieved.

Morphology

What about the morphology? The approaching velocity profile will collide with the pipe and cause the generation of a vortex on the upstream (or luff) side just as has been the case for piles and small objects. Since the horizontal pipeline presents a less streamlined shape to the flow (compared to the vertical pile), the upstream vortex may not be as nicely defined as the horseshoe vortex near a vertical pile. On the other hand, this vortex will be (theoretically) as long as the segment of exposed pipe.
Because the flow past the pipe cross-section is very unsymmetrical now, a larger and stronger (in comparison to that for a free-standing cylinder) vortex will be formed on the downstream (or lee) side of the pipe. It will be 'one-sided', too, in that it will rotate in only one direction: Clockwise if the flow is from left to right as shown in figure 14.17. For those who are not sailors, the terms luff and lee originally referred to the windward and leeward side (or edge) of a sailboat sail.

Luff and Lee Erosion The upstream vortex, with its high turbulence and sharp velocity gradients, will cause what is called **luff erosion** - a bit of a trench, often wider and shallower than that near a pile - on the upstream side of the pipe.
The downstream vortex, too, will cause erosion - now called **lee erosion** - resulting in another trench, now (obviously) on the downstream side. The resulting trenches are shown somewhat schematically in image 2 of figure 14.18. The series of images in this figure depict a whole series of pipeline self-burial steps.
As these two trenches develop, one can imagine that sand under the pipe becomes unstable and falls gradually into the trenches. This loose sand is easily washed away.

Tunnel Erosion Ultimately the remaining ridge of sand under the pipe can no longer support the pipe's weight and resist the hydrodynamic pressure differential between the upstream and downstream sides of the pipe as well; it fails, letting water flow under the pipe. This flow is initially squeezed between the pipe and the sea bed, restricting the formation of the boundary layer; see figure 14.18 part 3. Velocity gradients are then very high on the bed under the pipe so that there is also a very large bed shear stress. **Tunnel erosion** of material directly below the pipe can go quite fast! The high velocity flow now present under the pipe reduces the original upward lift force for two reasons: Less water flows over the pipe now, and the pressure on the bottom side of the pipe is reduced as a result of the high velocity now present there.

Pipeline Sag Looking at the pipeline as a structural element for a moment, the pipe segment loses its vertical support as soon as the soil under it fails and tunnel erosion starts. Shear forces in the pipe convey the weight of the suspended pipeline segment to adjacent segments increasing their load on the intact sea bed and stimulating their failure

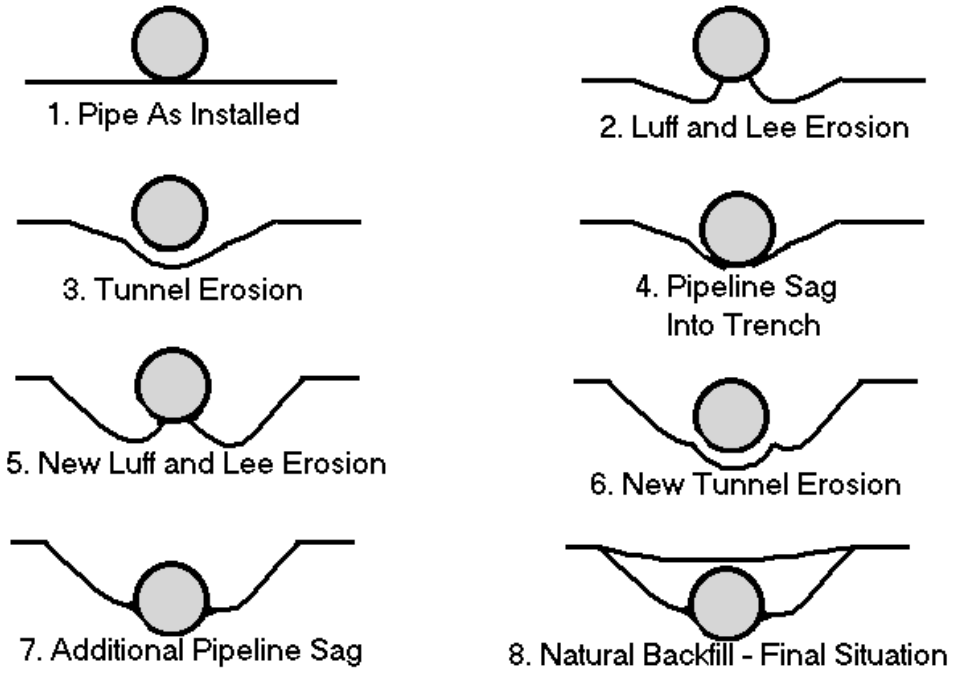

Figure 14.18: Pipeline Cross-Sections showing Progressive Self-Burial Steps

as well. The erosion tunnel can extend thus itself along the pipe axis crosswise to the flow. Obviously the pipe will start acting as beam, and as the erosion tunnel extends, the pipe will sag under its own weight into its own trench formed by the tunnel erosion.
In some cases the pipeline axis is nearly down to the original sea bed level (but still sticking up above the luff and lee erosion trenches) while a narrow tunnel still exists under the pipe. Ultimately, as the pipe continues to sink, it blocks less of the original flow thus reducing the driving force for the flow in the tunnel under the pipe. At the same time, the tunnel and streamlines under the pipe are getting longer, thus increasing the frictional resistance. At some point in this development, the current under the pipe will become too weak to transport (enough) sediment and the tunnel will become plugged with sand.

Repeated Cycle What happens next depends upon the extent to which the pipeline still projects above the sea bed. If the pipeline is high enough, luff and lee erosion will start again so that the entire cycle including a new tunnel erosion phase is repeated. Of course each repetition of this cycle leaves the pipeline a little lower relative to the original sea bed. If the pipe gets deep enough - often its crown is then even below the original sea bed level. Its disturbance to the flow will be so slight then that local erosion will stop and any remaining trenches will be re-filled by the ambient sediment transport. The final situation can be one in which the pipeline is completely buried and is even covered by a few decimeters of sand!

Tunnel Erosion Stimulation It is of course financially lucrative for a pipeline owner if this natural erosion process takes place; no costs are involved in this burial method! Since the costs of trenching and covering a pipeline can easily amount to several hundred guilders per meter of pipeline length, owners can be thankful for nature in this case! Dutch

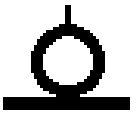

Figure 14.19: Pipeline with Spoiler

regulatory authorities are cooperative, too: They require that pipelines with diameters of 16 inches (406 mm) or less be buried only within a year after their installation. Since one good storm is often sufficient to completely bury a pipe line in Dutch waters, there is a good chance that this will occur - or, seen the other way, if it has not occurred within a year it probably won't occur at all. Then the owner will have to take action. The action that will have to be taken is discussed in a later section.

Why are owners only required to bury smaller lines? The reasoning is that smaller lines are weaker and can be more easily damaged by whatever may hit them - such as fishing gear, an anchor or something which has fallen overboard. Larger lines are considered to be strong enough. Also, since larger lines have a greater bending stiffness, they don't sag into their own erosion trenches as easily, either.
Do not get the impression that burial of a pipeline will actually provide that much protection against dragged anchors; anchors - especially those used in the offshore industry - usually dig in a bit too deep to pass over a pipeline. Expressed another way, most pipelines are not deep enough to escape a dragged anchor. On the other hand, pipelines are often buried more deeply - using artificial means - when their exposure to anchors is abnormally high - such as can be the case when a pipeline crosses a designated shipping channel.

Returning now to the main topic, how can the self-burial of a pipeline be stimulated? One obvious way would be to stimulate tunnel erosion by increasing the natural flow of water under the pipe. This can be done by blocking the flow of water over the pipe using what is often called a spoiler.
A pipeline **spoiler** is a vane, which typically sticks upright from the pipeline crown or top see figure 14.19. It usually projects about a quarter of the pipe diameter above the crown. The spoiler can be made of stiff but flexible plastic and it is held in place by plastic bands placed at intervals around the pipe. It is installed just before the pipeline leaves the laying ship during the installation process.
If the exposed pipeline and spoiler is hit by a towed object, it is designed to fold down temporarily and then spring back into its upright position.
Obviously the presence of the spoiler increases the drag force on the pipeline, but - once tunnel erosion has started - it makes the lift force even more negative so that the pipe is 'pulled' down toward the sea bed by the lift forces. This enhances its overall stability against sliding by increasing its normal on the soil elsewhere along the pipe.

14.9.2 Cover Layers

It has just been shown that natural processes can cause a pipeline or other small object to become buried in the sea bed. There are other situations in which it is desirable or even required that artificial means be used to cover or otherwise protect an object on the sea bed. Applications can be quite diverse:

- Cover an exposed pipeline or back-fill its trench,

- Locally cover a pipeline so that a new pipeline can cross it,
- Cover a long distance power or communications cable to protect it,
- Build up intermittent supports to prevent a pipeline from sagging too much into a deep 'valley' in the sea bed.

Most of these applications should be obvious. The last one has been used when crossing areas with hard and rough sea beds. The pipeline then tends to span from sea bed peak to sea bed peak. If this results in too long a span, internal pipeline forces can exceed allowable limits; an extra support is then needed. Such a support can be provided by a mound of coarse (stable) material installed at an intermediate location along the span. Of course the base of the support - up to the desired pipeline level - must be in place before the pipe is installed. Its top will be 10 meters or so square to allow some tolerance for the pipeline laying. After pipeline installation it is common practice to cover the pipe on top of the support mound in order to guarantee that it remains fixed at that location.
Two separate problems should become obvious to the reader from this discussion:

- How to guarantee the stability of a cover layer or intermediate support?
- How to install the necessary materials efficiently - especially in water depths of a few hundred meters?

These items will be discussed separately below.

Stability

In principle, the stability of any placed stone or gravel can be evaluated using the Shields criterion. A detailed review of the offshore situation, however, shows that conditions are not quite the same as in a river: The roughness of the dumped material will generally be different from that of the natural sea bed. Figure 14.20 shows such a situation rather schematically. This means that - at least at the upstream side - the approaching flow

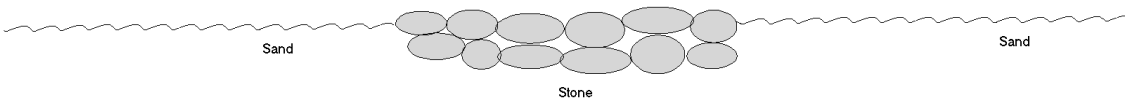

Figure 14.20: Cover Layer with Adjacent Sea Bed

velocity profile will be the one associated with the original sea bed roughness instead of the one that could be expected to develop above a bed of the dumped gravel or crushed stone. This velocity profile will probably generate a different shear stress as well. It should be obvious that at least the first part of the cover layer will have to remain stable under the influence of this latter (ambient) flow profile and resulting shear stress.
If the material placed on the sea bed distorts the general flow pattern as well - think of a berm or ridge of material covering an exposed pipeline - then the local influence of this flow distortion will have to be included in the analysis as well. Theory is often considered to be a bit too crude - still - for this sort of prediction; model tests are still popular for this. This has been (and can still be) an interesting experimental research area.
It has been pointed out that the stability of the first cover stones on the luff side can be critical. Is this the only concern? What about the start of the natural bed on the lee side? This bed is exposed to a velocity profile which has adapted (at least for the lower

few meters) to the roughness of the cover material. Assuming that the cover material is rougher than the sea bed - as will usually be the case - this flow may at least be a bit more turbulent than it would otherwise be. Local erosion of sea bed material on the lee side can often be expected. This means that the 'trailing edge' of the cover layer can be lost; it falls into the downstream erosion pit. This can be compensated very pragmatically by making the cover layer a bit wider. Then this loss will not be detrimental to the functionality of the cover layer.

Installation

It is one thing to design a local cover layer; one must still install it efficiently in a water depth of sometimes a several hundred meters. The hydraulic engineer's approach of just pushing gravel or stone overboard from a ship is fine for building a breakwater in shallow (from an offshore engineering point of view) water; it is not at all effective in deep water! In water deeper than a few tens of meters, cover layer material is often 'guided' toward the sea bed by a **fallpipe**. This is a long, more or less vertical pipe which extends from the work ship to a point just a few meters above where the material is to be deposited. The gravel or stone is then dumped into the top of the pipe; it will then come out the bottom a while later.

The fall pipe, itself, only really needs to contain the stone or gravel being dumped. It can be made up in at least three ways using either:

- 'Conventional' pipe sections - often made from plastic to save weight. This makes a closed pipe.
- A series of loosely coupled 'funnels' such as those used onshore to guide building renovation waste down into a container. Such a fallpipe allows water to enter at each joint.
- A 'loosely braided hose' made of chain links which contains the flow of solids. This is porous (to water) over its entire length.

Whatever type of fallpipe is used, it should be obvious (from chapter 12) that it will not simply hang straight down from the workship. Indeed, the combined action of the ship's forward speed plus any currents will exert quasi-static drag forces on the pipe, causing it to swing from the vertical. It may even respond to excitation coming from the ship's motion in waves as well. In order to be more certain that the lower end of the fall pipe is exactly in the desired position, that end is often equipped with a remote controlled vehicle or **spider**. This spider will have thrusters to compensate for small positioning errors.
The computation of the external hydrodynamic forces on a fallpipe is relatively straightforward. Even so, the prediction of its more complete static and dynamic behavior is not a trivial task. Attention, here, however, focuses on its internal hydraulics.

Internal Fallpipe Hydraulics Since the pipe is open at the bottom, it will fill with water as it is initially deployed from the work ship. It is convenient at first to consider an impermeable pipe and to keep its top end above the sea surface. The pipe will be filled to sea level with still water when material dumping starts.
The hydrostatic pressure in the surrounding sea water will match the static pressure resulting from the column of clear water or later even the mixture of water and gravel in the pipe. This is shown in figure 14.21. Since the stone or gravel dumped into the pipe will increase the overall density of the mixture in the pipe, this dumping will cause the

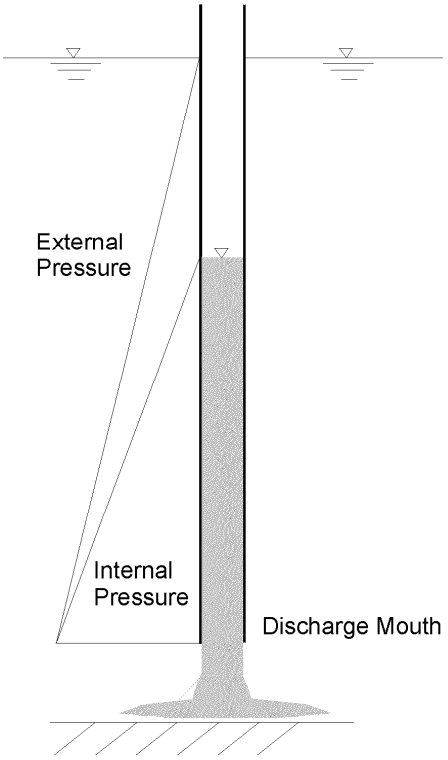

Figure 14.21: Pressure Distribution in and Around a Fallpipe (not to scale!)

liquid (mixture) level in the pipe to drop. The faster material is dumped into the pipe, the higher the concentration of solids in the water in the pipe. Thus, the overall density of the mixture will become higher, too. To compensate for this, the mixture level in the pipe will drop even more.
The upper segment of the pipe - at least - will be subjected to a substantial net external pressure as shown schematically in figure 14.21. This pressure difference forms a structural engineering problem for the pipe, but this may not be the biggest problem, however. With a constant rate of material dumping, the density of the mixture in the pipe will become constant and the *water* in the pipe will come to rest. This means that the stone or gravel dumped in the pipe will move downward in the pipe through essentially still water; it will move with its fall velocity - which is not especially high! The table below summarizes some typical soil grain fall velocity values (in water). This data can be found in chapter 4 as well.

Particle Type	**Sand Grain**	**Gravel**	**Stone**
Diameter (mm)	0,2	20	100
Fall Velocity (m/s)	0,02	1,0	2,35

The particles will fall relatively freely (and much faster) through the air in the pipe above the water; they will be abruptly decelerated by their impact with the water (lower) surface in the pipe. The only way the total mass transport of stone can be maintained with the sudden lower velocity is for there to be many more particles per unit length of pipe. If this 'concentration' becomes too high, the stone or gravel can bridge across the pipe and block

it so that nothing more gets through; this is a disaster for the productivity of the entire operation and embarrassing for the supervisor as well!
Even when this is working properly, the particles move relatively slowly - only with their fall velocity - through the still water in the fallpipe. It would be attractive to increase the productivity in terms of tons or cubic meters of solid material placed per hour using the same fallpipe.

One way to increase the productivity of the entire system is to let water flow down the fallpipe along with the stones. Since at any elevation the external hydrostatic pressure is greater than that in the pipe - see figure 14.21 - one has only to provide an opening to allow surrounding water to enter. This can be done at chosen intermediate elevations, at the top only, or even continuously along the pipe. One way to let the water enter is to use a porous pipe - such as the chain links hose - or simply to lower the top end of the pipe below sea level so that water overflows into it at the top.
Now, the particles sink through the moving water and a flow of water plus particles is discharged from the bottom end of the pipe. For the same rate of material supply as was used with the closed pipe, the concentration of particles discharged will be relatively lower and the discharge velocity will be higher when water is also moving downward through the fallpipe. Adding water is certainly a simple way to increase the productivity of the system, but how far can one go with this?

Discharge Morphology What can happen when too much water is allowed to enter the fall pipe? The discharge velocity gets so high that a vertical jet (of a mixture of water and solids) collides with the sea bed and spreads out. It has even happened that this local spreading current - with its higher density and thin boundary layer! - generates too much local bed shear stress for the material being deposited.. Discharged stone will be swept away from the place where it is wanted taking the reputation of the contractor with it!

Another interesting question involves the effect of the grain size distribution of the material. If all of the particles are essentially of the same size and density, then their fall velocities will be more or less the same, too. For some applications, such as insulating a hot flow line between a subsea well and a production platform, it is desirable to use a well graded gravel to cover the pipe. This reduces the permeability of the cover, thus reducing the heat loss from the pipe via convected sea water in its vicinity. (Some crude oils become semi-solid if they are cooled below their so-called pour point temperature; it can be very important for the pipeline operator to keep things warm!)
When a well graded mixture of gravel sizes is dumped into a fallpipe, then the coarse material will fall faster than the fines. This means that when a discharging operation is started, first only coarse material will be discharged; there will be a 'tail' of fines at the end of the run as well. This need not be important - of itself - for a long pipeline, but it can make a mess of an attempt to form a neat supporting mound of material by passing slowly back and forth to build it up.
A second complication when discharging a well graded mixture of gravel is that the finest material must remain stable on the sea bed in the discharge jet. Segregation of the particles can take place so that coarse material is left near the pipeline with the finer fractions deposited more to the sides. This can mean disaster for the insulation function of the cover layer. It has led to litigation between the pipeline owner and covering contractor in the past.